Dual Fuel Combustion and Hybrid Electric Powertrains as potential solution to achieve 2025 Emissions Targets in Medium Duty Trucks Sector

Energy Conversion and Management
Volume 224, 15 November 2020, 113320
https://doi.org/10.1016/j.enconman.2020.113320

Antonio García[a], Javier Monsalve-Serrano[*, a], Santiago Martinez-Boggio[a], Patrick Gaillard[b], Olivier Poussin[c] and Amer A. Amer[d]

[a]CMT - Motores Térmicos, Universitat Politècnica de València, Camino de Vera s/n, 46022 Valencia, Spain
[b]Aramco Fuel Research Center, Aramco Overseas Company B.V. Paris, France
[c]VOLVO Group Trucks Technology, 99 Route de Lyon, 69806 Saint Priest, France
[d]Fuel Technology R&D Division, Saudi Aramco Research & Development Center (R&DC), Dhahran, Saudi Arabia

Corresponding author (*):
Dr. Javier Monsalve-Serrano (jamonse1@mot.urpv.es)
Phone: +34 963876559
Fax: +34 963876559

Abstract

The European commission is targeting a 15% reduction in CO2 emissions for medium and heavy-duty transportation starting in 2025. Moreover, the next European normative (EU VII) will impose a decrease of 50% for NOx and particulate matter emissions with respect to the current EUVI normative. Meeting these requirements pose a significant challenge to truck and bus manufacturers. Several proposals appeared in the last few years as improve the cabin aerodynamics, decrease the friction losses and improve the powertrain efficiency. The last point involves improving the current combustion systems as well as the transmission and energy management. This work proposes to couple two potential technologies to reduce at the same time the global (CO_2) and local pollution (NOx and soot). For this, two truck platforms representative of medium-duty applications (18 ton and 25 ton) are tested using the reactivity controlled compression ignition (RCCI) combustion mode with diesel and gasoline as fuels. In addition, the trucks are electrified to full hybrid technology in a parallel pre-transmission (P2) architecture. A 0D vehicle numerical model is used to evaluate the trucks under four different driving cycles representative of homologation and real driving conditions. The numerical model is validated against on road measurements. The RCCI combustion is modeled by means of a map-based approach with 54 points measured in steady-state conditions. This work presents a complete engine map calibration with measurements up to 350 hp using two combustion modes inside the map (so-called dual-mode dual-fuel). As a baseline, the commercial diesel no-hybrid trucks and the dual-fuel no-hybrid trucks are used. The results show the potential of the dual-mode dual-fuel combustion to achieve ultra-low NOx and soot emissions. In addition, the CO_2 target reduction is achieved for several truck platforms and driving conditions due to the hybridization of the driveline. The cycles with large phases of urban driving are the most favorable due to the ability of recovering energy by means of the regenerative braking system and the possibility to avoid large idling phases with respect to the no-hybrid versions. In addition, the decrease of the payload improves the CO_2 reduction with respect to the baseline cases

Keywords

RCCI, Hybrid powertrain, Emissions regulations, Driving cycles

1. Introduction

Zero Emission Vehicles (ZEV) including Battery (BEV) and Fuel Cell electric vehicles (FCEV) can address the Tank to Wheel CO_2 target mandates and address air quality concerns in city centers. The opportunity for increased market penetration over the coming decades is entirely possible, as a result, for light-duty applications. These opportunities do not lend themselves naturally to the Medium- and Heavy-Duty (MD and HD) truck applications, due the prohibitive battery weight and size that impact the payload and total cost of ownership as a result – critical factor for fleet operators and owners of such vehicles. ZEV technologies for MD and HD are restricted to vehicles where conventional diesels are not allowed (e.g. city centers) [1]. Therefore, opportunities to reduce the fuel consumption while meeting or beating future CO_2 is becoming an emerging research field, particularly because the growth in energy demand over the coming decades is coming from these applications [2]. The goods transport applications are expected to manage a conflicting set of the requirements including vehicle gross weight, travel routes, final use and individual trip distance [3]. Currently, the fueling infrastructure for ZEVs (e.g. high-speed electric charging and H_2 filling stations) is limited to LD application presenting another impediment for mass deployment of these technologies for trucks applications [4]. In addition, increasingly more stringent regulations on pollutant emissions such as NOx and soot are prevalent [5]. Given all these constrains, the main question is how to achieve the desired targets for 2025 (15% of CO_2 reduction) in MD and HD applications.

Hybrid electric vehicles (HEVs) were studied for more than 15 years in passenger car applications, and they are currently a mature technology being commercially available at a large scale [6]. In a first level, it can be distinguished between full HEV and plug-in HEV depending on the possibility of re-charging the battery from the electric grid. In a second level, it can be also differentiated between series, parallel and series-parallel depending on the powertrain architecture. Despite the great improvements in the recent years in terms of efficiency and durability, the information about the advantage and drawbacks in truck platforms is very limited [7]. Parallel architecture is one of the most used powertrain layouts due to the reduce amount of change necessary with respect to a conventional powertrain and the use of one electric machine instead of two as other architectures. The position of the electric machine in the powertrain defines the typology of the parallel architecture. P0 is called when is inserted in the place of the alternator and the maximum power is reduced (<15 kW). P1 and P2 are two layouts with the electric machine between the ICE and the transmission. The difference between them is that for P2 a clutch is inserted to allows pure electric vehicle driving. Lastly P3 refers to electric machine after the transmission. P2 is the most used due to the capacity to operate in pure electric mode and multiplied the torque by the transmission when is necessary. However, for medium and heavy duty trucks the manufacturers only offer prototype versions or market-specific solutions for primarily urban travel. Among the works found in the bibliography [8–11] related to good transportation trucks and buses, Smallbone et al. [2] showed a comparison between different heavy-duty powertrain configurations. In the cited work, a conventional powertrain fueled with diesel and hydrogen, as well as a FCEV and BEV were analyzed among others. The work shows that the energy vector and its primary energy source are the most important factor in reducing the global CO_2. The pure electric truck platform offers no direct tailpipe emissions. However, it produces significantly worse life cycle CO_2 emissions than a conventional diesel powertrain. In turn, it is demonstrated that there is no appropriate common powertrain solution for all the vehicle types. Other important factor is the final use of the vehicle. It is a large difference between medium-duty urban and rural applications and heavy-duty with mainly highway routes. According to the simulation results of Lajunen [12], the fuel economy of a HD vehicle (40 to 90 ton) with parallel powertrain can be improved by up to 6% with respect to a conventional powertrain. This work also indicates that the HEV is more beneficial in operating routes that have more hill climbing. Warey et al. [13] studied a Class 2 truck (12 ton) with improvements in CO_2 of 2.5% for micro-hybrid (start/stop functionality), 13% for a P1 and 20% for a P2. The maximum improvement in tailpipe CO_2 emissions was the high-voltage series-parallel hybrid with a 25% CO_2 improvement with respect to the diesel no-hybrid truck. Lastly, the work of Banjac et. al [8] features the characteristics of test cycles leading to better energy conversion efficiency of hybrid trucks. The results of the cited work show that the hybrid trucks only enable a fuel consumption reduction in the cycles in which the conventional powertrains feature low efficiency of the ICE, and also in those with large braking phases. Apart from the mentioned works, focused on applications intended for goods transportation, there is a lack of information about the benefits of electrified powertrains for different truck applications and none using low temperature combustion modes to power the vehicle. In addition, almost all the works found in the literature are focused in the fuel economy and CO_2 reduction, without analyzing other pollutant emissions.

The larger emissions restrictions rise the necessity of studying active ways to decrease the harmful components in the tailpipe gas. In addition, the hybrid operation with large amount of start and stops events makes the aftertreatment systems (ATS) operation even more difficult due to the low exhaust temperatures. To overcome this point, the addition of e-components as e-heaters in the exhaust line could help. Another possibility is to prevent the emissions of these noxious species by avoiding its generation during the combustion event. Several authors are studying the application of low temperature combustion modes (LTC) for compression ignition engines (CI) [14–16]. This concept is a promising advanced combustion strategy for reducing both NOx and soot emissions simultaneously, with a beneficial effect on the fuel economy [17]. Several concepts can be found in the literature beyond the LTC approach [18]: homogeneous charge compression ignition (HCCI), partially premixed combustion (PPC), premixed charge compression ignition (PCCI), reactivity controlled compression ignition (RCCI) and gasoline compression ignition (GCI). The main differences among these combustion strategies are related to the fuel injection timing and fuel composition. The RCCI concept uses two fuels with different reactivity to control the ignition timing and the heat release rate profile. Similar to diesel engines, HCCI, PPC and PCCI engines use only one fuel, but promoting early injection timings to ensure a sufficient air-fuel mixing before the combustion to avoid the soot production [19]. Along the years, several works were performed with different fuels and control strategies. However, all of them found as main limitation the impossibility to achieve an entire engine map calibration suitable for real applications. Sun et al. [20] developed a 6.4L V8 HCCI engine and control system for a hydraulic hybrid shuttle bus. The calibration map can achieve diesel-like efficiencies and low NOx emissions without ATS. However, reducing HC and CO emissions remains as challenge. Other major problem is the maximum power that can be achieved. In the cited work, 30% less power than that of the diesel engine was achieved due to cooling and air management restrictions. Solouk et al. [21] developed a multi-mode LTC-SI engine operating with HCCI at low engine speed and low-medium load, RCCI at medium engine speed and all the load range, and conventional SI for the rest of the map. With 70 hp (120 Nm at 4000 rpm) of maximum power, the concept was applied in a D-segment passenger car with P2 HEV. The results show the fuel economy benefits with respect to the conventional SI map and the LTC time use. The last-mentioned parameter increases from 8% to 21% by reducing the vehicle electrification level from PHEV to MHEV. To overcome the difficulties to achieve high engine loads, Benajes et al. [22] proposed a multi-mode combustion concept moving from a fully premixed combustion (as RCCI) at low loads towards a diffusive dual-fuel one at high loads. The multi-mode combustion concept allows the dual-fuel operation in the whole engine map; however, some calibration constraints as NOx and soot emissions must be relaxed [19]. Additionally, as the combustion strategy shifts towards to a diffusive one, the engine efficiency decreases as a consequence of the higher combustion duration [20]. Therefore, during the engine calibration it is intended to obtain the maximum percentage of the engine map operating with a premixed combustion. The literature review of Pachiannan [18] reveals that the major concerns in LTC are related to the combustion control over a wide range of loads and the CO and HC emissions. In addition, it is addressed the lack of work that asses the complete vehicle evaluation with this type of combustion modes (performance, fuel consumption and emissions).

In this work, a dual-mode dual-fuel (DMDF) combustion mode is used to evaluate two hybrid electric truck platforms (18 and 25 ton of payload) that cover the medium-duty market in Europe. A complete calibration map for a 350 hp 8L CI multi-cylinder engine is achieved by using RCCI combustion up to medium load and dual-fuel diffusion at high load. A P2 parallel pre-transmission hybrid powertrain layout is used and optimized to achieve ultra-low NOx and soot emissions together with a CO_2 reduction with respect to the conventional commercial truck. The truck platforms are evaluated by means of a 0-D vehicle model in different driving cycles representative of homologation and real driving conditions. The validation of the results was performed using data from on-road tests in both commercial no-hybrid truck platforms. The aim of this work is to evaluate the potential of combining the two technologies, LTC and hybridization, to achieve the 2025 European targets. A cost analysis is included in order to balance the CO_2 penalties and battery cost for the right sizing of the components.

2. Background and Novelty of the Current Study

Compression ignition engines are used in medium- and heavy-duty applications due to the higher efficiency (low carbon dioxide) than spark ignition engines thank to their unthrottled charging, lean combustion and high compression ratio. As was seen in the

Diesel-gate case, the main concerns for these vehicles continue being the NOx and particulate matter (mainly soot) emissions associated to the high combustion temperatures (high compression ratio) and fuel-rich regions (DI diffusion combustion). This study goes beyond the current state-of-the-art by considering LTC modes and hybrid electric powertrains for a range of truck platforms. The aim of this study is to evaluate the potential of the abovementioned technologies in homologation and real driving conditions to achieve the 2025 targets. Specifically, it focuses on the potential of high efficiency RCCI calibration map fueled with diesel and gasoline in a P2 FHEV powertrain for decarbonizing the good transportation sector and their sensitivities. It presents a novel method to design, select and evaluate electrified powertrains for truck applications. In addition, the information presented in this work is useful for future performance estimation and help researchers and manufacturers to support decision making across the whole vehicle development strategy. The outcomes indicate what performance may be possible in future generations of goods transportation vehicle technology. Results show the potential of RCCI hybrid powertrains to improve fuel economy and achieve NOx and soot emissions below the legislation at engine-out levels.

3. Methodology

The evaluation of two truck platforms representative of medium-duty applications using RCCI and dual-fuel diffusion LTC combustion modes in a parallel full hybrid powertrain was performed in a numerical 0-D vehicle model. The model was fed with experimental results obtained in several test beds to reproduce with accuracy the ICE, vehicle and battery behavior. The numerical model was validated for the commercial no-hybrid vehicle in on-road conditions. The methodology applied to design, test and post-process the results are explained in the next subsections.

3.1. Vehicle numerical model

The vehicle 0-D model was developed in the GT-Suite commercial software (v2020, Gama Technology) for two truck platforms with 18 and 25 ton of maximum payload. These trucks are representative of the European medium-duty sector for goods transportation in urban and extra-urban conditions. Figure 1 shows the two vehicles under study and Table 1 depicts their main specifications. The trucks are named as FL (18-ton max payload) and FE (25-ton max payload) and originally equipped with an 8L six-cylinder diesel engine in two versions: FL with maximum power of 280 hp and FE with maximum power of 350 hp. Both trucks use an ATS system composed of a Selective Catalytic Reduction – SCR urea (NOx reduction), Diesel Oxidation Catalyst - DOC (HC and CO reduction) and Diesel particle filter - DPF (soot filtration) for achieving the current EU VI normative. In the current work, the 8L six-cylinder original engine was used for the two trucks with several modifications to allow the dual-mode dual-fuel operation. The main constrain used along the present work was to achieve the same performance than the commercial truck (maximum power and torque output). Therefore, as was described in the introduction, the goal is to reduce the engine-out emissions, particularly NOx and soot, as well as the tailpipe CO_2 emissions with the proposed technologies.

FL 280 hp 18 ton FE 350 hp 25 ton

Figure 1- Truck platforms representative of medium-duty applications used for vehicle analysis.

Table 1 – Main vehicle specifications for 0-D model trucks of the commercial version FL and FE medium duty Volvo Trucks [23].

Parameter	**FL truck**	**FE truck**
Base vehicle Mass [kg]	5240	7035
Max Payload [kg]	12760	17965
Vehicle Drag Coefficient [-]	0.65	
Frontal Area [m^2]	5.52	6.89
Rolling friction [-]	0.0155	
Tires Size [mm/%/inch]	295/80/22.5	295/80/22.5
Gear Box [-]	6 gears	12 gears
Differential ratio [-]	5.29	3.08
ICE rated power [hp]	$280_{@2100rpm}$	$350_{@2200rpm}$
ICE rated Torque [Nm]	1050	1400

To assemble the parallel P2 pre-transmission hybrid electric truck model, a battery pack and one electric machine (EM) were added in the driveline with models obtained from the bibliography. The resistive forces (aerodynamic, friction, road slope, etc.) for both truck platforms were validated with on-road measurements with the commercial no-hybrid version.

As mentioned, a P2 full hybrid powertrain was used. Figure 2 shows a scheme of the proposed P2 dual-mode dual-fuel hybrid truck concept. One motor/generator is added between the ICE and the OEM transmission. Moreover, a battery pack and all the power electronic systems with the inverter and signals conditioner is also added. It is important to note the addition of one extra fuel tank to feed the secondary injection system with gasoline fuel. The main reasons to select a P2 architecture was due to the small changes compared to the original powertrain [24]. A full hybrid selection was done instead of micro- or mild-hybrid due to the hard targets set for 2025 (15% CO_2 reduction) and the necessary power that is needed to compensate the de-rated ICE with the RCCI calibration.

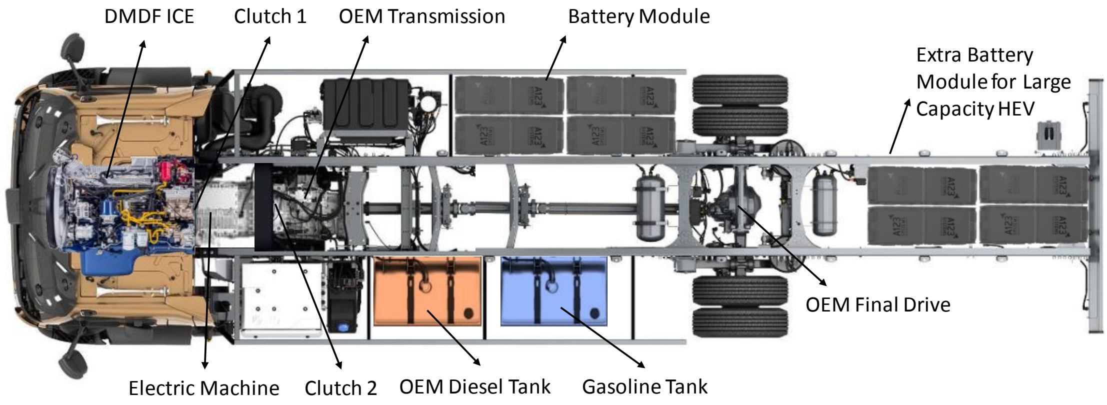

Figure 2 - P2 parallel pre-transmission DMDF Truck concept.

The control system was done using a rule-based control (RBC) strategy due to the online application possibility and its robustness [25]. In a parallel architecture controlled by an RBC system, four different modes can be identified. Pure electric mode, in which the electric machine propels the vehicle with the engine turned off. The second mode is battery charging, in which the ICE is turned on to propel the vehicle and charge the battery. In this case, the EM operates as generator. The third mode is the boost mode, in which both the ICE and EM deliver power to propel the vehicle. The maximum powertrain brake torque is achieved in this mode. The last mode is regenerative braking, in which the ICE is turned off and the EM operates as generator. To control the operative mode at each instant, rules are used to switch between modes and to decide the split of the energy in the case of battery charging (second mode) or boost mode (third mode). More information about the RBC strategy can be found in [26].

The value for the rules, RBC parameters, were calibrated in the optimization section. The first parameter is the maximum vehicle speed at which the operation mode changes from pure electric (generally used at low vehicle speed) to hybrid mode. By disengaging the clutch 1 (Figure 2), the EM propels the vehicle with the ICE switched-off. Therefore, pure electric travel with zero tailpipe emissions can be performed. This operating mode is mainly used in urban areas, helping to the local pollution reduction and avoiding excessive ICE start and stop. The second parameter is the boost mode split ratio, which divides the required torque between the ICE and EM. Moreover, the battery needs to be recharged in order to return the SOC to the initial value. From the charging mode, two additional parameters arise. The first one corresponds to the SOC value to start the battery charging. This determines the energy window (from $SOC_{initial}$ to SOC_{charge}) in which the battery must operate. The second parameter is the intensity at which the battery is charged. For this, a PID in which the proportional gain was set as a function of the maximum EM power and the SOC limit is used. When SOC_{actual} is equal to SOC_{limit}, the maximum EM machine is used to recharge the battery. For conditions in which the SOC_{actual} is greater than the SOC_{limit}, a proportional value is used. As a full hybrid, the battery state of the charge (SOC) needs to be the same at the initial and at the end of the driving cycle. A tolerance of 1% of the total energy of the cycle was set to accept or discard the control configuration. Moreover, the deviation of the target vehicle speed was also considered with a maximum accumulative deviation of 3% in the total distance.

The last control parameter is the gear shift strategy. This is a crucial point due to its notable impact on the ICE and EM operation speeds. The gear shift was optimized by a single parameter that stablishes the rotational speed at the input of the transmission (ICE and EM rotational speed) at which the gear changes. Depending on the truck platform, a six (FL 18-ton) or twelve (FE-25ton) gear automatic transmission is used. The parameter was swept between the minimum and maximum allowed speed of the ICE.

In terms of hardware, the battery package size (energy content) is also optimized. This has a direct impact on the pure electric mode range, the vehicle flexibility to operate along the different modes and the power losses. As shown in Figure A1 (appendix A) the increase of the battery total energy reduces the current through the cells and with this the columbic losses. On the contrary, this has a disadvantage in terms of the total battery weight and cost. All these aspects are addressed along the work. The cell type and materials selection, as well as the cell arrangement are also difficult tasks due to the several options found in the market. For this work, cylindrical cells of Li-FePO4 produced by A123 Systems were used due to the maturity of its application in the automotive field as well as by its reliability in terms of safety issues when compared to higher energy density lithium-cells. Forgoez et al. [27] studied the battery behavior under several ambient temperatures and discharge and charge loads. These data allowed to create a detailed electrical and thermal model for the battery pack.

The electrical circuit model was built starting from the cell model and then expanded with several cells in parallel and series arrangement (Figure 3a). For each cell, an equivalent electrical circuit model based on a Thevenin circuit with one resistance and two parallel resistor-capacitor sub-circuits in series was used (Figure 3b). The last component allows to model the electrical dynamics of the cell (i.e. diffusion processes), even though it does not consider the hysteresis effects, which were not modelled due to the lack of data. The dependence on temperature and SOC of all the resistances and capacitors present in the model, both for discharge and charge operations, is formulated according to the work by Perez et al. [28]. The main cell and battery pack characteristics are detailed in Table 2. The selection of the battery pack voltage (600 V) was done to reduce electrical losses in the truck electrical circuit (mainly wirings) and to facilitate the control of the electric machine. As was demonstrated by [29], the battery package nominal voltage selection cannot be done from a battery perspective. It is important to note that in this work the total battery capacity is optimized by means of a DoE with a range between 4 and 54 parallel cells (7-80 kWh). Therefore, the total number of cells are presented in the results section. In terms of battery weight, this means between 50 kg to 700 kg plus the packaging and electric components. The extra wright has less impact for truck applications than for passenger cars because it only represents 1%-11% at empty truck and 0.2 to 3% at full payload.

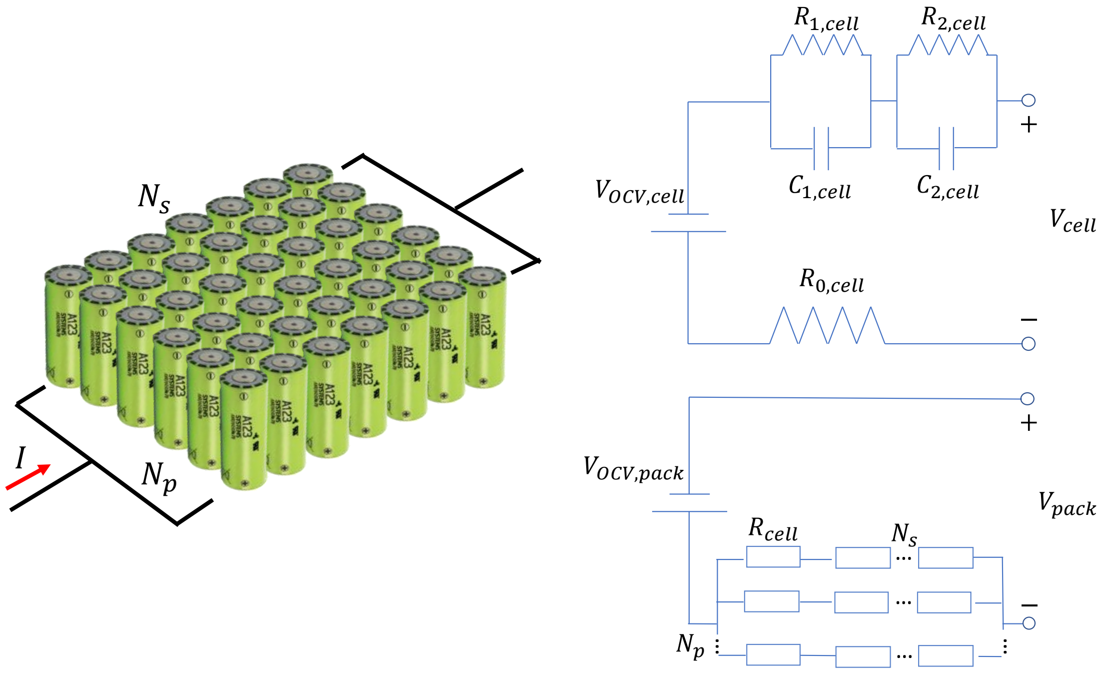

(a) (b)

Figure 3- Cells arrangements in a battery pack (a) and electric circuit model with one cell (top-b) and the all pack (bottom-b).

Table 2 – Li-Ion battery cell A123 26650 LiFePO4 and 600V battery pack main specifications.

Cell Technology	LiFePO4 (manufactured by A123 Systems)	
Cell Open Circuit Voltage	[V]	3.3
Cell Capacity	[Ah]	2.5
Cell weight	[kg]	0.076
Battery packaging	[kg]	20% of total cells weight
Battery Open Circuit Voltage	[V]	600
Number of Series cells	[-]	181
Max current to charge	[A]	$120_{@10s}$ & $70_{@continuous}$
Max current to discharge	[A]	50
Max voltage	[V]	3.61
Min voltage	[V]	2.01

The electric machine is the other main electric component that needs to be added in the hybrid P2 vehicle model. In this powertrain layout, it operates as a traction motor in the pure electric and boost mode (positive torque). In addition, it is used during the regenerative braking and battery charging modes for recover the deliver battery energy (negative torque). In the P2 architecture, the EM speed is always positive (same rotational direction than the ICE). To build the EM model, a map-based approach with an efficiency map against speed and torque and the maximum and minimum speed-torque curve was used. The JMAG motor design tool is an open source software generally used to develop the EM model [30]. JMAG is a parameter-based motor design support tool. It has the ability to evaluate all the motor characteristics like torque-speed characteristics, loss characteristics and inductance characteristics, among others. Specifically, a three-phase induction motor inner rotor and distributed winding cage was used. In this work, two EM with maximum power of 70 hp and 140 hp were used. Figure 4 shows the EM layout and efficiency map with the respective maximum and minimum torque output and speed. The JMAG considered an EM weight with a power-to-mass ratio of 2.5 kW/kg. This value is taken from [31] as an average value of several EM manufacturers.

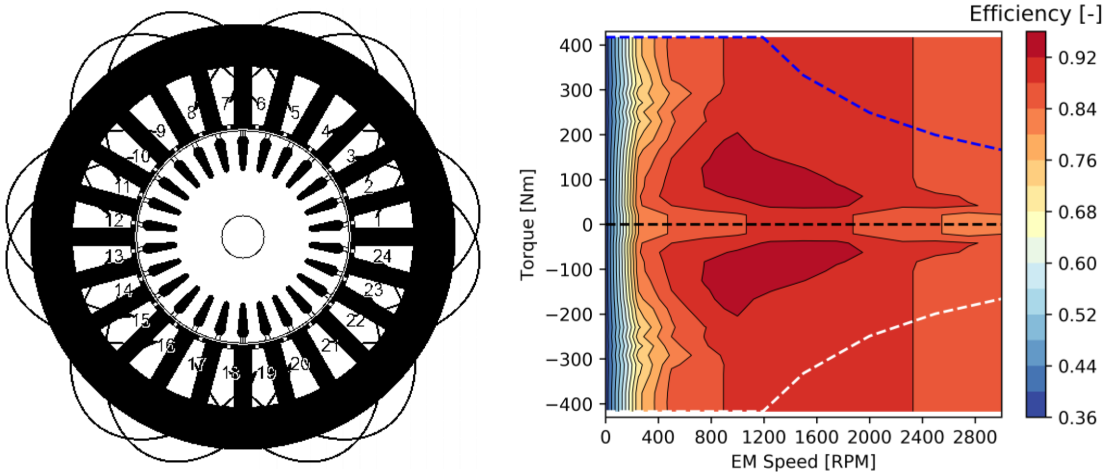

(a) (b)

Figure 4 - Electric machine circuit scheme (a) and efficiency map (b) for EM 70 hp version.

All the above-mentioned control and hardware parameters are tested with a Latin Hypercube design of experiment (DoE) with 1500 cases for each case is used. A summary of the parameters and their respective range tested is shown in Table 3. More information about the optimization parameters and the RBC control programming can be found in [32,33].

Table 3 – DoE optimization parameters

Parameter	Type of parameters	Range Tested
Battery Size	Hardware	7 - 80 kWh
Gear shift Strategy	Control Transmission	1300 - 2200 RPM
Max Pure Electric mode	Control Electric machine	5 - 120 km/h
Boost mode split	Control Electric machine	0 – 100 %
SOC start charge	Control Battery pack	0.45 – 0.58
SOC maximum charge	Control Battery pack	0.45 – 0.58

3.2. Internal combustion engine characterization

Through the different LTC concepts, the RCCI combustion can be highlighted as one of the most promising concepts due to the balance between fuel consumption, emissions and operating range [34]. This concept is based on using two fuels with different reactivity, allowing to tailor the reaction rate by modifying the amount injected of each fuel. This provides a greater control degree on the combustion development compared to other concepts as the HCCI, which relies only in the in-cylinder conditions and the reactivity of a single fuel [35]. In spite of being easier to control, the use of a low reactivity fuel, as gasoline, can bring problems at high loads. If high EGR rates and a correct combustion phasing cannot be achieved, the pressure rise rate can be excessive and the mechanical integrity of the engine can be compromised. In addition, the high EGR rates can lead to soot formation problems. Therefore, in the previous years, the research group proposed a dual-mode dual-fuel combustion [36], in which RCCI is used at low and medium load and a dual-fuel diffusion combustion is promoted at high load (see Figure 5a). The transition zone is coupled with an intermediate injection strategy between the two aforementioned modes, called highly premixed RCCI.

The injection strategy of the two fuels, diesel (DI, marked with green) and gasoline (PFI, marked with blue) are illustrated in Figure 5a. At low-to-medium engine load, two high reactivity fuel (HRF, Diesel) injections were used following the principles of the fully premixed RCCI combustion: a first injection to increase the reactivity of the mixture near to the cylinder wall and a second injection to provide ignitable regions; both being early injections in the compression stroke. Nonetheless, as the engine load was increased towards the full load operation, the high-pressure gradients required a modification of the injection strategy. In this mode, called dual-fuel diffusion, the diesel pilot injection was removed as it provided an instantaneous ignition of the mixture. In this sense, the diesel injection was concentrated in one injection to increase the amount of fuel and provide more energy release by the diffusive combustion process. To achieve this diffusive combustion, the start of injection was shifted towards the TDC fire. However, the use of this strategy enhances the soot production and the NOx emissions. The first is a result of the premixing decrease, producing rich mixture zones. This diffusive combustion process also extends the combustion duration, which means that the nitrogen molecules have higher residence times at high temperatures. Therefore, these conditions require to relax the emissions constraints to allow achieving higher engine loads. An intermediate zone was reached in the map, called highly premixed RCCI, in which the diesel injection pilot is maintained but the main injection is displaced towards TDC fire. For all modes, as the low reactivity fuel (LRF, gasoline) is injected in PFI, the injection timing is located in the intake stroke.

Figure 5b shows the effect of the different injection strategies in the mixture formation on an equivalence ratio-temperature map, where the NOx and soot formation peninsulas are highlighted. These data was extracted from previous work by means of CFD analysis [37]. More information about the calibration procedure can be found in [36].

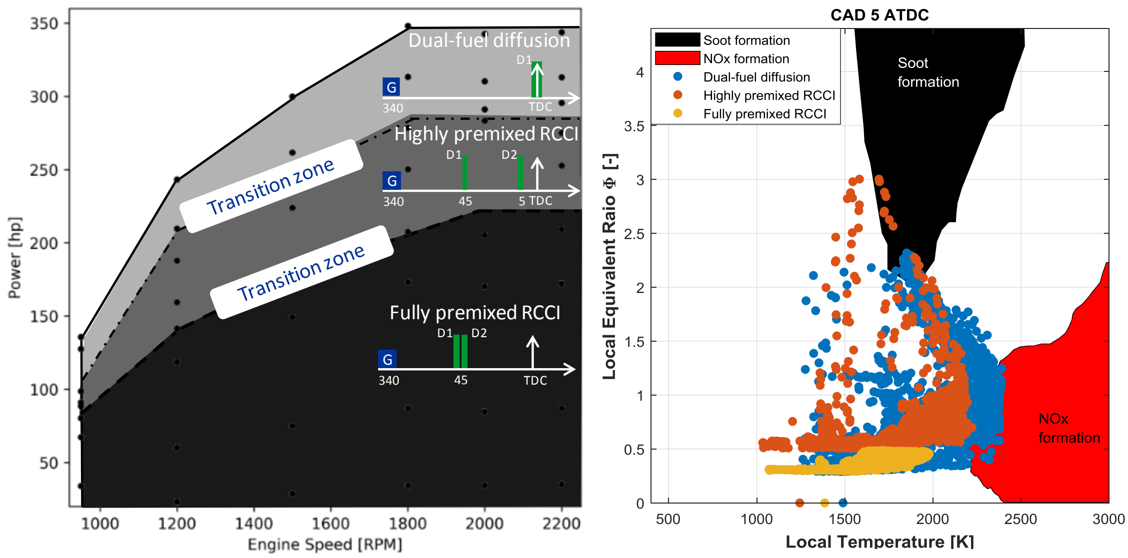

(a) (b)

Figure 5 – Calibration strategy with combustion types by power and rotational engine speed (a) and example of 5 CAD ATDC local equivalent ratio and local temperature distribution for the three phases (b).

The internal combustion engine used in this work is a medium-duty 8L six-cylinder engine originally calibrated for diesel operation. The main characteristics of the OEM and DMDF ICE are detailed in Table 4. To transform the CI diesel engine to a dual-fuel LTC engine, several modifications were performed. First, six PFI gasoline injectors were added in the intake manifold. Second, a low pressure EGR (LP-EGR) line was installed to complement the high pressure EGR (HP-EGR) line. The first line takes the exhaust gases after the turbine and the second line before the turbine. This makes that both systems have different pressure and temperatures. A mixture of both systems helps to control the combustion chamber temperature and ICE efficiency. Finally, the piston bowl was modified for RCCI operation, having different geometry and compression ratio (4.8 points lower) than the stock one. The optimization details of these parameters can be found in [38]. Additionally, the engine control unit was modified to operate with the new injection strategy as well as the modified air management system. The ICE was fully instrumented for the engine test campaign. In this sense, six-cylinder pressure sensors (Kistler 6125C) to measure in-cylinder pressure together with temperature (thermocouple type K) and pressure transducers (Kistler 4045A) were added in the intake, exhaust, lubrication and cooling circuits. The CO_2, CO, HC and NOx emissions were measured with a HORIBA-MEXA 7100 DEGR and the soot measurements were done with an AVL 415 smoke meter.

Table 4 – Main engine specifications used in the three truck platforms

Parameter	CDC ICE	DMDF ICE
Type	4 stoke, 4 valves	
Nº Cylinders	6	
Displaced Volume [cm^3]	7700	
Stroke [mm]	135	
Bore [mm]	110	
Injection type	DI diesel	DI diesel -PFI gasoline
Compression ratio [-]	17.5	12.8
High pressure EGR	Yes	Yes
Low pressure EGR	No	Yes
Turbo Configuration	VGT	
Rated Power [hp]	$352_{@1800rpm}$	$348_{@1800rpm}$
Rated Torque [Nm]	1453	1444

The reference maximum rated outputs presented in Table 4 were measured in the experimental campaign. The DMDF achieved the same maximum power and torque values than the original CDC calibration. This is a key point for the vehicle application in the next sections. The fuel consumption and emissions were measured in 52 operating conditions between 950 and 2200 rpm and 15-350 hp (black points in Figure 6). The measurements of the same operational points were repeated with the OEM configuration (CDC ICE) for a fair comparison. Figure 6a and Figure 6b show the fuel consumption map and the CO_2 emissions at tailpipe conditions, respectively. It is preferred to present tailpipe instead of engine-out values due to the emission legislation requirements. The estimation was done by measuring the CO_2 emissions at engine-out conditions and converting all the CO and HC to CO_2. The gasoline fraction (GF, $m_{gasoline}/m_{Diesel} + m_{gasoline}$) and EGR levels used in the calibration are illustrated in Figure B1. The highest fuel economy (below 200 g/kWh) was achieved at medium load and speed due to the flexibility of this map zone to increase the GF (>80%) and EGR rate.

Figure 7 shows that this zone achieved the lowest NOx value (0.2 g/kWh) with almost negligible soot emissions. In the transition zone, see Figure 5, the soot emission increases gradually with the load. However, the NOx emissions remain below 0.4 g/kWh, which corresponds to the tailpipe EU VI limit for heavy-duty applications. The fuel economy in this region is acceptable with values around 205 to 210 g/kWh. The GF rate decreases due to the high-pressure gradients down to values around 60%.

Lastly, the dual-fuel diffusion zone completes the engine map up to 350 hp with lower GF rates (<50%) than the previous zone. In this zone, the engine load is given by the diesel fuel instead of the gasoline, as was in the RCCI and transition zone. It is important to note that due to the similar lower heating value of both fuels, the gasoline fraction is equivalent to the premix energy ratio (PER, $m_{gasolineLHV_{gasoline}}/m_{Diesel}LHV_{diesel} + m_{gasolineLHV_{gasoline}}$). In the highest load zone, the calibration was performed to achieve NOx emissions below 2 g/kWh and the soot emissions below 100 mg/kWh. For reference, the CDC calibration map achieves values of 9 g/kWh for NOx and 60 mg/kWh for soot. It is important to remark that the CR decrease (see Table 4) has a strong effect on the calibration results. For one side, it allows to achieve an entire calibration map with dual-fuel combustion and ultra-low NOx values in a multi-cylinder engine. The in-cylinder conditions are not possible to control as single-cylinder prototypes. On the other side, the fuel economy achieves values close to the CDC ICE but cannot be further improved. As it is well known, the CR has a direct impact in the brake thermal efficiency. In spite of this, the differences are lower than 7 g/kWh (200 g/kWh for DMDF and 193 g/kWh for CDC). The CO and HC emissions are illustrated in Figure B2. The LTC modes has large CO and HC emissions due to low temperature combustion inside the combustion chamber and the PFI gasoline injection. However, at was demonstrated in previous works, the measured values can be converted with market DOC without major problems [39].

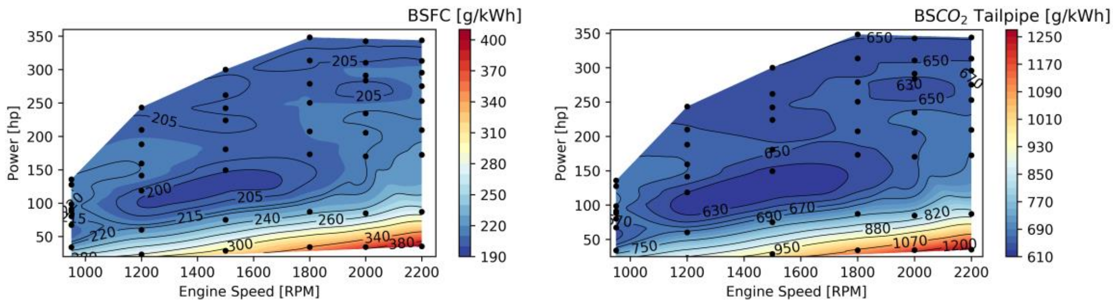

(a) (b)

Figure 6- Dual Fuel dual mode brake specific fuel consumption map (a) and brake specific CO2 tailpipe emissions map (b).

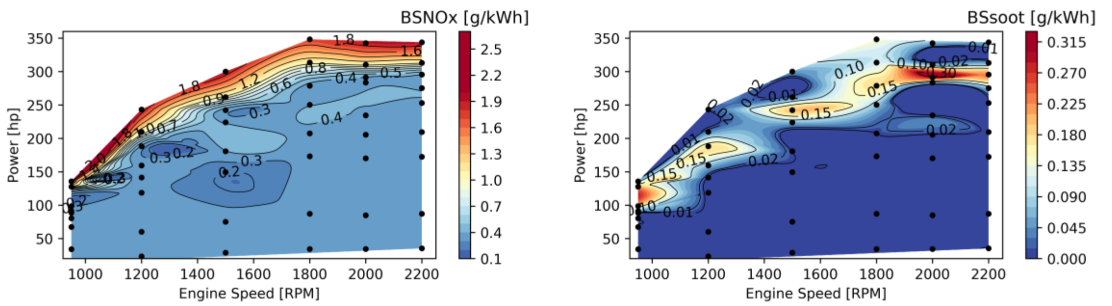

(a) (b)

Figure 7- Dual Fuel dual mode brake specific NOx emissions map (a) and brake specific soot emissions map (b).

Figure 8 summarizes the emission maps highlighting the zones in which the EU VI normative for stationary conditions is fulfilled for NOx and soot (0.4 g/kWh and 0.01 g/kWh, respectively). The three zones defined with dashed lines correspond to three engine calibration maps used in the different truck platforms along the work. The de-rating methodology is widely used by heavy-duty engine manufacturers to reduce the amount of engine versions in the different truck applications. In this work, the calibration zone in which is possible to achieve the EU VI NOx and soot levels simultaneously in the complete region will be referred to RCCI 210. The nomenclature allows to identify the main combustion mode and the maximum power output in horse power. One step further is the DMDF 280, being EU VI compliant only in NOx for the complete map. Finally, the DMDF 350 is the complete map calibration presented above.

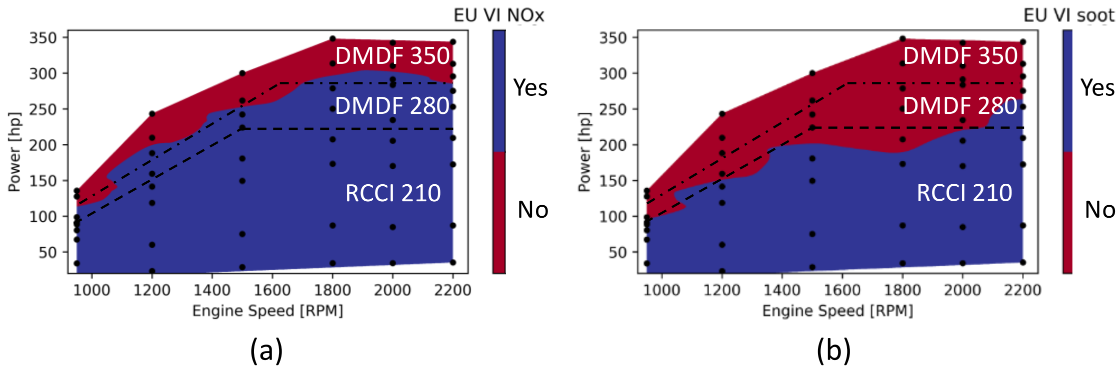

Figure 8- Dual Fuel dual mode EU VI normative comparison for NOx (a) and soot (b).

3.3. Driving cycles

The two truck platforms showed in Figure 1 were studied in transient conditions trough the numerical 0D-vehicle model. The transient conditions selected were different driving cycles that represent homologation conditions, as the WHVC and real driving emissions. The data to model the last-mentioned cycles was taken in real routes through a GPS in a no-hybrid commercial diesel Truck. The driving cycles selected for this study represent combined cycles with initial urban area, and later a rural and highway phases. Only one of the cycles does not contain the highway phase (Figure 9b). Therefore, it was called Urban Hilly. It is important to note that altitude measurements were considered in the real driving cycles. For the WHVC, the altitude is zero due to the homologation specifications. Moreover, the duration and total distance of the real driving conditions are larger than the WHVC. The real driving cycles used in the current work are extensively used by the OEM of the considered no-hybrid truck during the truck development phase and performance study. The vehicle speed and altitude data against the time for the different driving cycles is shown in Table 5.

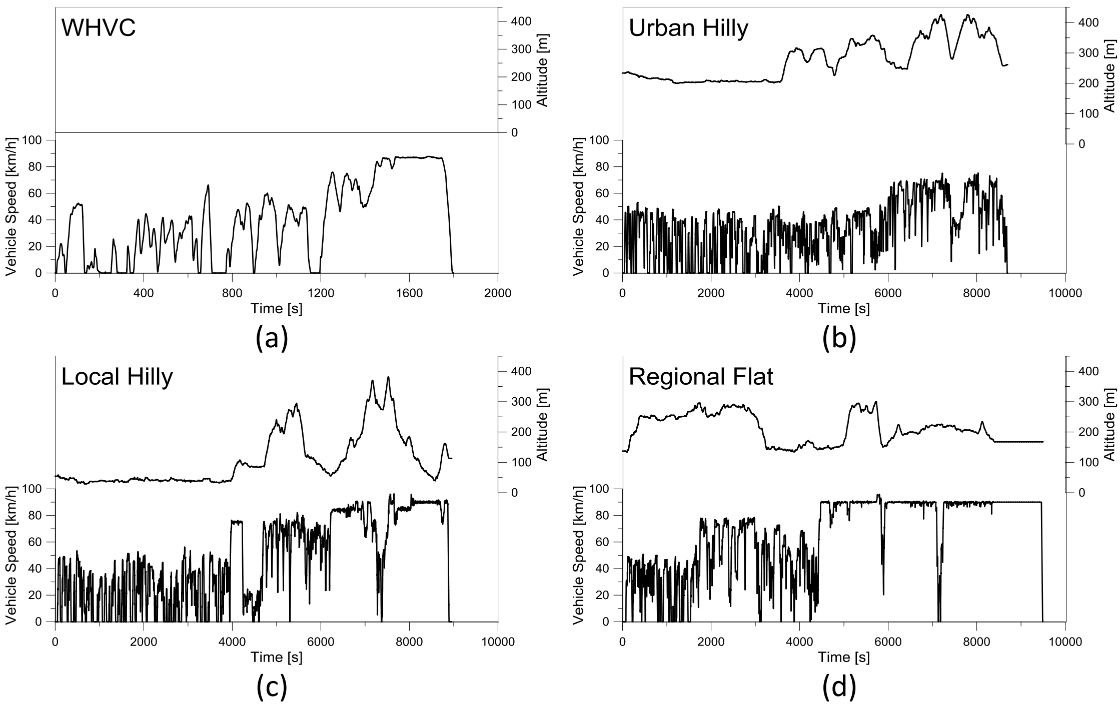

Figure 9- Homologation and real driving cycles with vehicle speed and altitude against time.

Table 5 – Driving cycle main characteristics

Parameter	WHVC	Urban Hilly	Local Hilly	Regional Flat
Time [min]	30	145	138	158
Distance [km]	20	85	119	176
Max Speed [km/h]	88	75	96	96
Avg Speed [km/h]	40	35	48	66
Acc time [%]	46	29	29	20
Dec time [%]	32	21	24	16
Stop time [%]	26	12	13	4
Cruising [%]	28	38	34	61
RPA [m/s^2]	0.09	0.12	0.10	0.06

The regenerative braking is one of the key aspects that needs to be considered and studied when a hybrid electric vehicle is under evaluation. The parallel hybrid braking system retains all the major components of the conventional mechanical brakes and adds the electric machine braking torque on the rear axle. A preliminary analysis was done through the speed versus deceleration probability graphs. Figure 10 shows the post-processing of the data acquired during the WHVC driving cycle. Figure 10a depicts the operative points in braking situation (only negative acceleration) against the vehicle speed. Later, these points are passed to a probability color map in Figure 10b. The lines included in the graphs correspond to the braking power calculated with the vehicle forces for the case of FE 25-ton truck and 100% payload. Finally, the Figure 10c shows the real available braking energy that can be recovered due to vehicle balance restrictions. The rear brakes in a truck cannot deliver the 100% of the power during a deceleration phase. The Economic Commission of Europe (ECE) stablishes a brake regulation, which indicates the minimum braking force on the rear wheels. In addition, Bao et al. [40] developed an optimum braking split between the rear and front wheels which is known as I-Curve that meets the legislation requirements and improves the regenerative braking. This gives the maximum braking force that makes the front and rear wheels lock simultaneously for each friction coefficient. When the braking force is distributed to the front and rear wheels on the I-Curve, safe braking is assured. For both truck platforms the I-Curve distribution is around 65% for rear axles and 35% for the front axles. This split was used in Figure 10c to evaluate the potential of regenerative braking.

Figure 11 shows the other three driving cycles and the corresponding maximum recovery energy as Figure 10c. The Urban and Local cycles were the cycles that show high probability of braking occurrence for powers higher than 35 hp. The rest of the cycles concentrate the decelerations at low load and high speed. It is important to note that the maximum regenerative braking is limited by the maximum EM power (full line in Figure 10 and Figure 11). The high density of points of almost all the cycles in the low deceleration region (low brake power) and the required split between the front and rear axles will cause in the P2 hybrid architecture that the increase of the sizing of the electric machine will not bring high benefits.

Additional limitation in the braking system is added as battery maximum power and SOC limitation for the battery safe. In addition, below 5 km/h the truck does not recover energy due to a safety limitation. All these points have a direct impact on the fuel consumption and are considered in the result analysis.

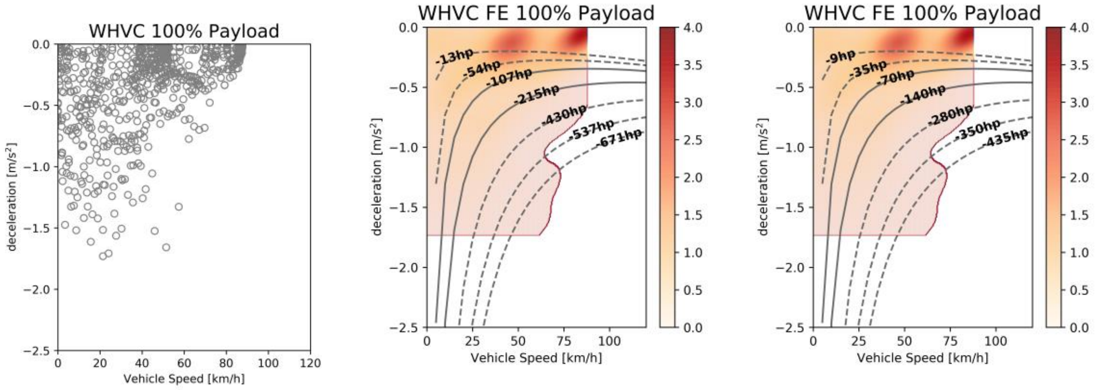

(a) (b) (c)

Figure 10 – Regenerative braking analysis for FE 25ton truck in WHVC and 100% of payload. Post-processing analysis with working points (a), frequency map plus potential regenerative braking (b) and frequency map plus real potential regenerative braking (c).

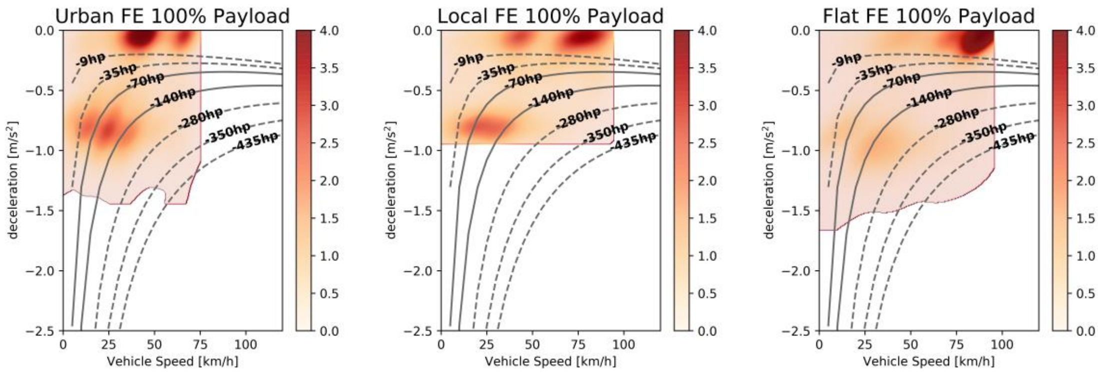

(a) (b) (c)

Figure 11 – Real regenerative braking analysis for FE 25ton truck in real driving cycles and 100% of payload.

3.4. Model Validation

The 0D-vehicle model with all the powertrain components were validated against on-route measurements. A commercial FE 25-ton no-hybrid diesel truck platform was tested with torque measurements in the ICE and output of the transmission, gear position, fuel consumption, engine data (rotation speed, driver acceleration demand) and GPS data (speed, acceleration, altitude) against the time. Figure 12 shows the truck platform with the different measurement sensors position. The torque measurement in the ICE and transmission output axle allows to calibrate the transmission and clutch losses as well as the transient behavior of the components. The fuel consumption was compared against the simulation results. All the real driving cycles showed in Figure 9 were performed.

The model calibration allows to check the vehicle information collected previously in Table 1 and adjust the power losses in the transmission and the differential. For the ICE modeling, the measured map of fuel consumption with the 54 operative points for CDC was used. This allows to validate the map-based approach used in this work for the DMDF combustion. Figure 13 shows the instantaneous and accumulated fuel consumption mass of diesel with the experimental and simulation results for the Local Hilly cycle. The model allows a good agreement in terms of total fuel consumption with a deviation below 2%. Moreover, Figure 13 shows a good agreement in the transient behavior with similar peaks. The rest of cycles show similar agreements and are not included for the brevity of the manuscript.

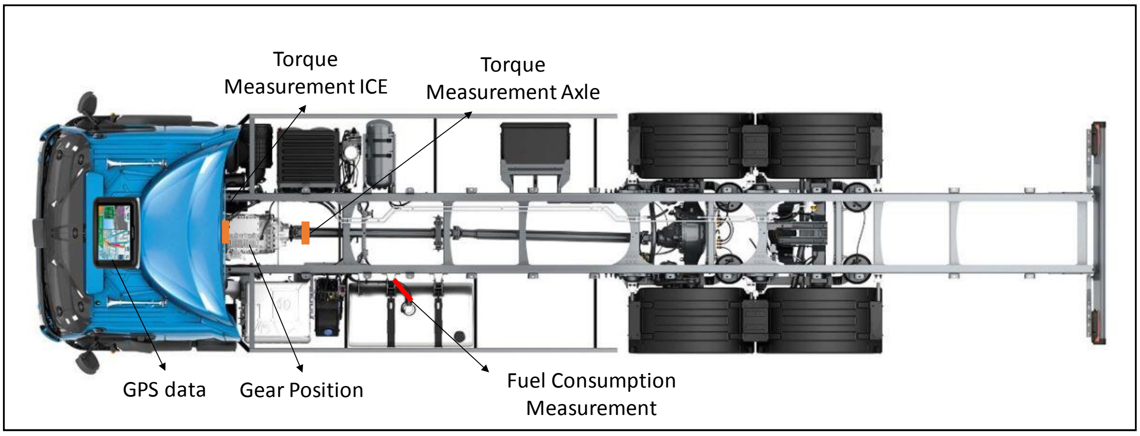

Figure 12- FE 25-ton CDC no-hybrid powertrain layout and sensor position for on-route fuel consumption measurements.

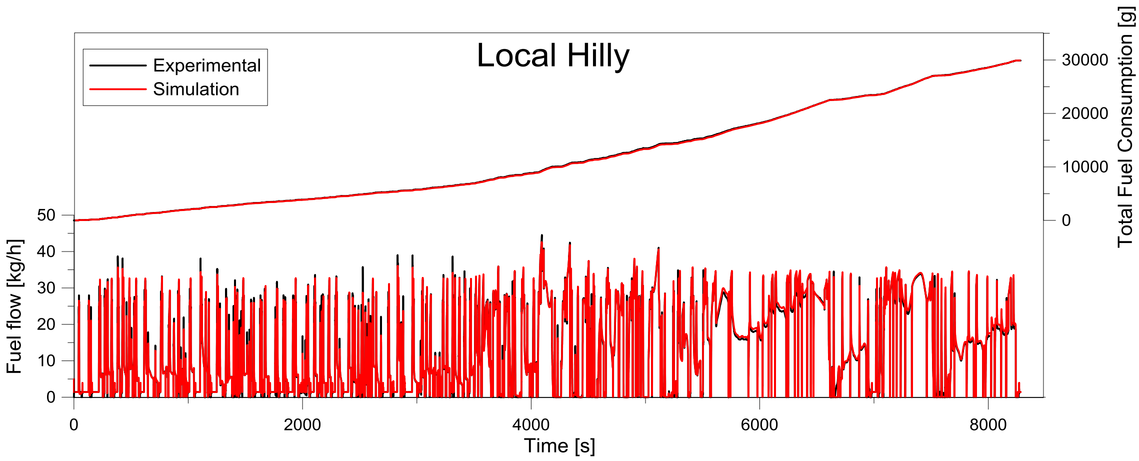

Figure 13 – Total and rate of fuel consumption against time for the Local Hilly driving cycle measured with the FE 25-ton CDC no-hybrid truck with 50% of payload.

After validating the conventional vehicle simulation model, the hybrid P2 was built in the same model basis but with all the electric components and new controllers. In addition, the ICE maps were substituted by the DMDF ones. The main target of the results is to investigate the impact of hybridization on not only fuel consumption, but also the exhaust behavior like the raw emissions. Due to difficulties to measure the emissions in a route, it was not possible perform comparisons in this sense. However, in a previous work for a light duty vehicle [32], the authors validated also the emissions for a similar approach of the current work.

3.5. Optimization Approach

This study deals with two truck platforms with maximum power output of 280 hp and 350 hp and three possible LTC map versions: RCCI 210 hp, DMDF 280 hp and DMDF 350 hp. This scenario allows several combinations between the trucks and ICE maps. As was shown in the experimental section, the map measurements show that as lower is the maximum power ICE output the lower are the NOx and soot emissions. The main assumption to assembly the test matrix is that the maximum total power output must be equal to the commercial diesel no-hybrid version. Therefore, Figure 14 shows the different hybrid P2 versions for each truck platform and the baseline cases for comparison. The electric machine is sized to compensate the ICE power and achieve the same maximum power than the commercial diesel platform.

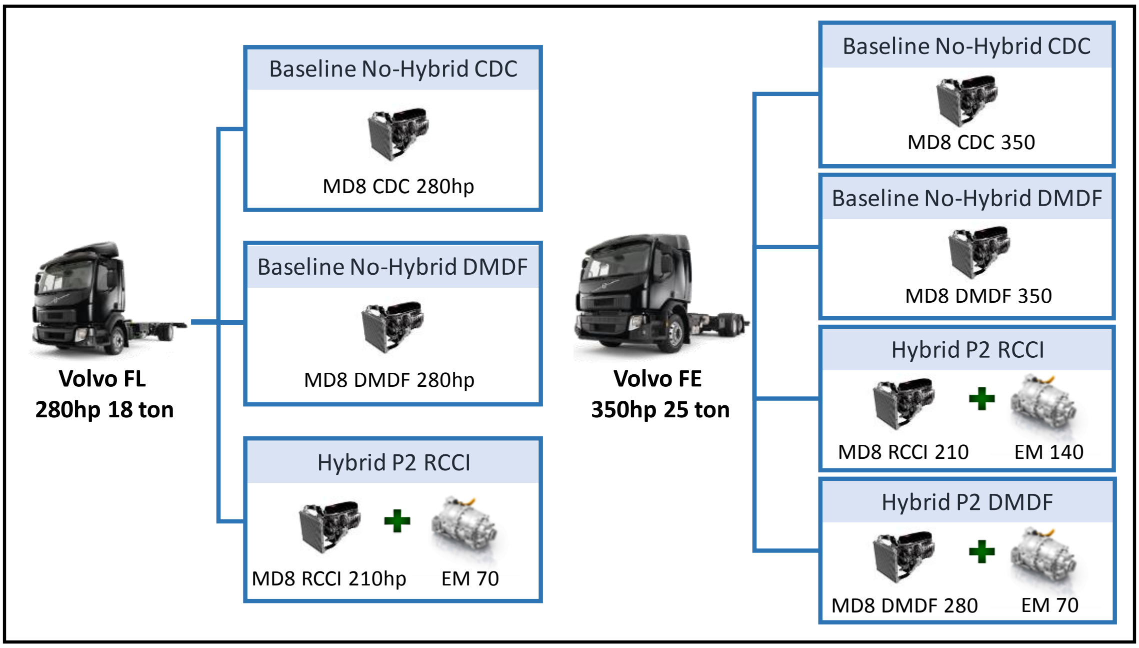

Figure 14 – P2 hybrid versions and baseline references scheme.

For each truck platform configuration, an optimization methodology is applied. In particular, three payload conditions (0%, 50% and 100% relative to the maximum payload) and four driving cycles are considered. This methodology leads to 12 possible cases to study, as shown in Figure 15 (left scheme). From the 12 cases, only those corresponding to the WHVC (inside the red rectangle) are used to in the DoE to optimize the vehicle components. For each hybrid option, 4500 (1500 x 3 payloads) cases were simulated, leading to around 13500 (4500 x 3 hybrid versions) total simulated cases. For the optimization, only the WHVC (Figure 15a) was considered due to two main reasons: 1) This homologation cycle was created to represent average conditions around the world and it is the unique cycle used for European homologation and 2) After a sensitivity analysis, it was seen that the payload has a greater impact on the component and control selection than the driving cycle characteristics. Two optimization criteria are considered to select the best case of the DoE results:

- To achieve the lowest possible CO_2 emissions for the three payloads (WHVC 0%, WHVC 50% and WHVC 100%).
- To minimize a cost function that considers the battery cost and the European CO_2 penalties expected to 2025 in payload homologation conditions (WHVC 50%).

Therefore, four single optimums (WHVC 0% min_{CO2}, WHVC 50% min_{CO2}, WHVC 100% min_{CO2} and WHVC 50% min_{cost}) are obtained. Finally, these single optimums are tested for the complete matrix (12 conditions) leading to four sub-matrixes (Figure 15b).

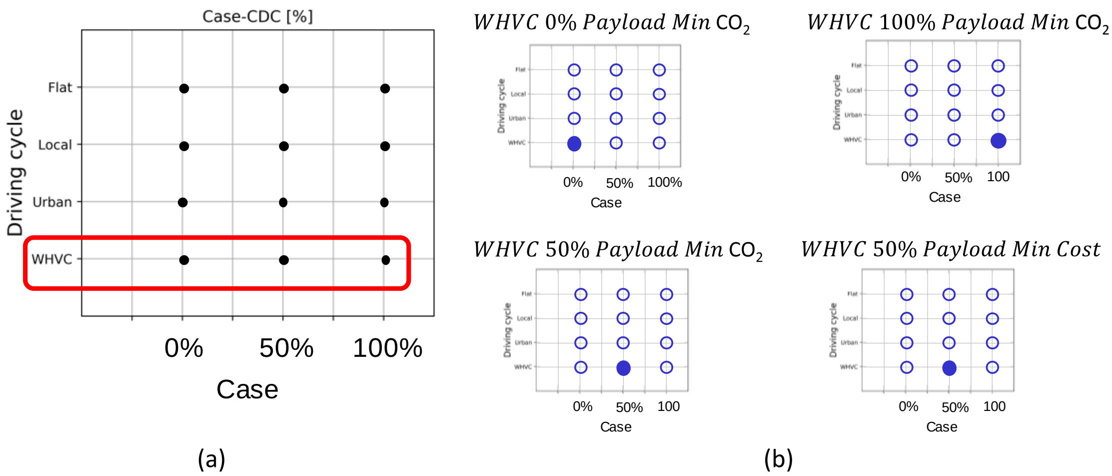

Figure 15 – Optimization strategy with 12 simulated cases (a) and the 4 matrix for the selection of the optimum case (b).

To apply the second optimization criterion, it is necessary to stablish an estimation for the CO_2 benefits and components cost. For the first item, the European Commission stablishes a CO_2 reduction target for 2025 and also a monetary penalty for companies that exceed this target. The targets are expressed as a percentage reduction of CO_2 emissions compared to the EU average in the reference period from 1 July 2019 to 30 June 2020. For 2025, the CO_2 reduction target is 15%. The financial penalties in case of non-compliance of the CO_2 targets is set to 4250 € per g/tkm (grams per ton and kilometer) of CO_2 in 2025. In this work, the average of the current no-hybrid analyzed fleet (FL 18-ton and FE 25-ton CDC no-hybrid) is taken as reference in the homologation cycle (WHVC) at normative conditions (50% payload). The vehicle weight taken for the CO_2 calculation is the 50% of the payload in the case of the no-hybrid platform. Therefore, the total vehicle tons are the sum of the cargo mass at 50% plus the vehicle and electric components weight. The cost function is expressed with Eq (1).

$$f_{cost}[€] = CO_{2@penalty}[€] + Battery\ Cost\ [€] \tag{1a}$$

$$CO_{2@penalty}\ [€] = (CO_{2@2025}\ [\frac{g}{tkm}] - CO_{2@case}\ [\frac{g}{tkm}]) * 4250[€/\frac{g}{tkm}] \tag{1b}$$

with $CO_{2@2025}$ 15% lower than the $CO_{2@2020}$ of CDC no-hybrid average fleet. The battery cost was estimated with the U.S. Department of Energy estimations with two scenarios [41]. The current average price of a lithium-ion pack (176 €/kWh) and the estimation for 2025 pack (100 €/kWh).

To determine the global optimum configuration, the average gain for each sub-matrix depicted in Figure 15b is calculated. Then, the global optimum is the case with minimum average CO_2 emissions among the different sub-matrix. A summary of the current methodology developed to optimize two truck hybrid powertrains is presented in Figure 16.

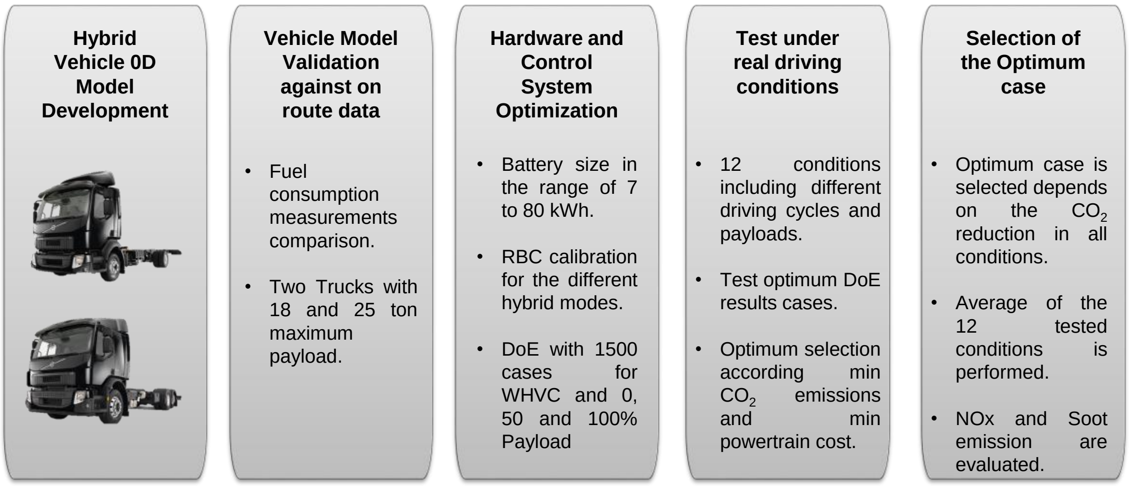

Figure 16 – Flow chart scheme of the methodology use to optimize two medium-duty truck platforms under dual fuel dual mode and reactivity controlled compression ignition combustion mode.

4. Results and discussion

The results section is divided into two subsections. Section 4.1 shows the influence of the parameters considered in the DoE optimization on the CO_2, NOx and soot emissions. Moreover, this section describes the selection of the optimum hybrid truck configuration considering the minimum possible CO_2 emissions. Section 4.2 explains the selection of the optimum configuration on a cost basis considering two scenarios of battery cost (years 2020 and 2025) and the European 2025 CO_2 penalties. Finally, the results of the single optimum configurations tested with different payloads and real driving cycles are presented. The results for both truck platforms are presented separately and then compared to have a global picture of the available trucks in the European goods transport sector.

4.1. Influence of the different parameters and optimum selection by maximum CO_2 reduction

Figure 17 shows the battery size against the CO_2 reduction for the three different payloads in the case of the FL 18-ton hybrid truck. The minimum allowed battery size for this platform is 7 kWh considering the need for a 70 hp electric machine (see Figure A2). As a multi-parametric analysis, the vertical points represent the effect of the rest of the parameters included in the DoE for a give battery size. On the other hand, the maximum CO_2 reduction for each battery configuration (Pareto frontier) represents the best point for each battery size. Thus, this frontier helps to understand the net impact of a given parameter on the output analyzed. From Figure 17, it can be inferred that the effect of the battery size on the CO_2 reduction is higher when the payload is reduced. As an example, 10 kWh shows 23% of reduction at empty truck, 17% at medium payload and 12% at full payload. This result can be explained by an increase in the ICE operation efficiency when the payload increases. In this sense, the CDC no-hybrid truck operates at higher engine loads, zone where the diesel combustion has a high efficiency (BTE>40%). Therefore, the electrification potential reduces with the increase of the payload, and with this the use of the electric machine. It is important to note that the minimum CO_2 emissions case for each payload is marked with a cross mark in the different subfigures. These cases are then taken as single optimums to analyze their behavior in other driving cycles and payload conditions.

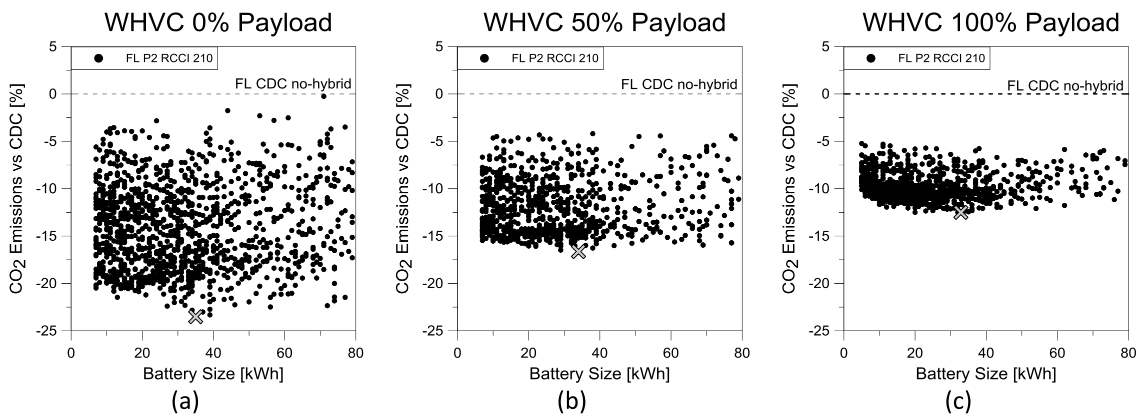

Figure 17 – Battery energy for P2 FL 18-ton truck against the CO_2 reduction compared to CDC no-hybrid for 0% (a), 50% (b) and 100% (c) payload.

The parameter with the highest impact on the CO_2 emissions reduction was the gear shift strategy (Figure 18). The range analyzed for this parameter was between 1300 – 2200 rpm, zone in which the RCCI calibration can achieve a range of ICE brake power between 180 hp - 210 hp (see Figure 8). The complementary power is delivered by the electric machine to achieve the nominal 280 hp of the CDC calibration. The high impact of the gear strategy can be seen by the strong change in the CO_2 reduction when the rotational speeds are changed. The decrease of the gear rotational speed improves the benefits in CO_2 due to the possibility to work at high engine loads. The same behavior can be observed in no-hybrid powertrains. However, the advantage of the P2 architecture is the possibility to electrically boost the engine when necessary and to maintain a low gear strategy. For medium and full payload, the fuel consumption (CO_2 emission) starts to increase below 1400 rpm due to the excessive EM boost use by the lack of ICE power. The best configuration for all payloads was found to be around 1500 rpm. It expected that for future trucks with more complex control systems and online data in terms of payload and route will improve the change between pre-calibration strategies. For this work, a fix calibration is used for all payload in the optimum selection section.

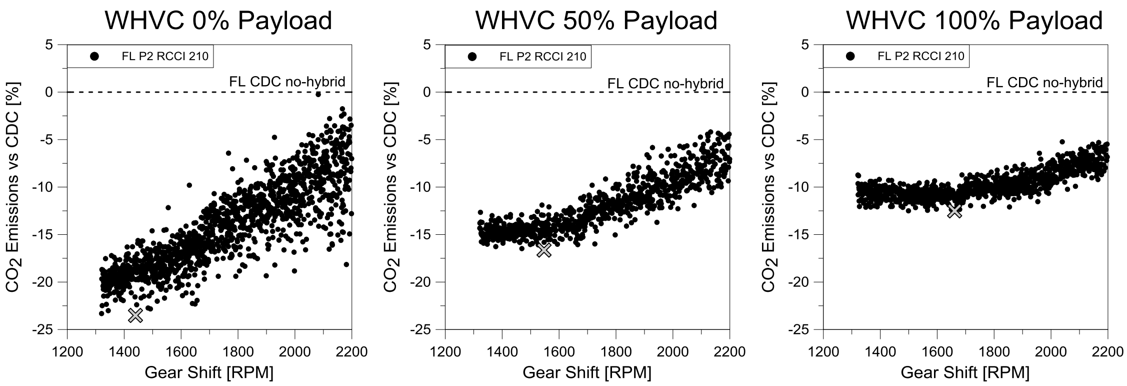

(a) (b) (c)

Figure 18 – Gear shift strategy for P2 FL 18-ton truck against the CO_2 reduction compared to CDC no-hybrid for 0% (a), 50% (b) and 100% (c) payload.

The effect of the other optimization parameters on the CO_2 emissions was found to be less important. The trend is flat with variation of the CO_2 reductions against the baseline case below 1% when the parameter is changed in the DoE. Figure 19a shows the split between the ICE and the EM in the boost mode. This mode is used when the battery SOC is above the SOC_{charge} (not necessary to charge the battery) and the vehicle speed is higher than the maximum one for the pure EV mode. The value of zero represents that all the power is provided by the ICE and a value equal to one means that the EM provides all the power in the boost mode. For 50% of payload, the trend is not clear and can be said that it is not a key parameter for the P2. In addition, Figure 19b shows the maximum vehicle speed at which the truck operates as a pure electric one. The width of the points is reduced with the increase of this parameter. However, a value close to the minimum CO_2 (maximum benefit) can be found for all the cases. Therefore, the maximum vehicle speed for pure EV mode is also considered a not important value. It is important to highlight that if the value is below the SOC charge, the vehicle will not operate as pure electric whatever the vehicle speed. Lastly, it is the SOC_{charge} (Figure 19c) that determines the window between the vehicle battery discharge and charge ($SOC_{initial}$ and SOC_{charge}). Again, as the previous two parameters presented, the Pareto frontier has a flat trend with not drastically CO_2 change with the variation of the parameter calibration.

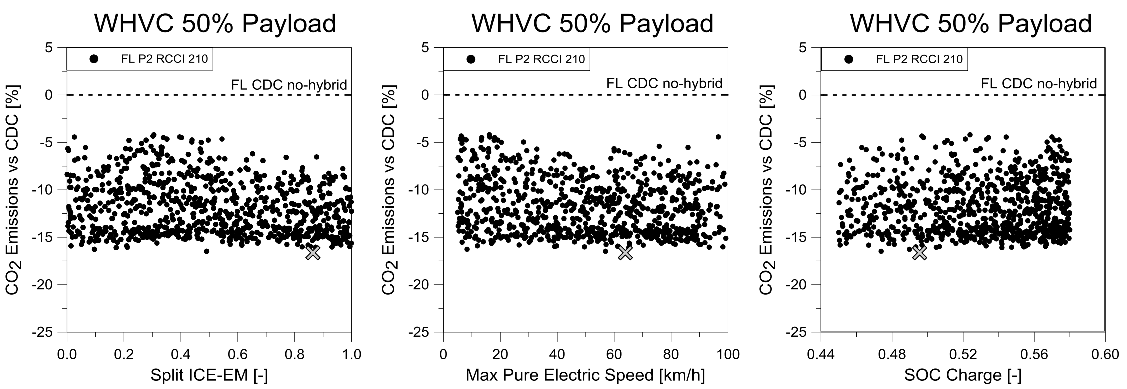

(a) (b) (c)

Figure 19 - P2 FL 18-ton truck at 50% payload CO_2 reduction compared to CDC no-hybrid for different split between ICE and EM (a), maximum pure electric speed (b) and minimum state of the charge to start battery charging (c).

The NOx and soot values are the other two main outputs of the model and there are considered in the optimization process. For the case of the RCCI calibration (map up to 210 hp) it is possible to achieve EU VI NOx (0.46 g/kWh) and soot (10 mg/kWh) in transient conditions. Figure 20 shows the NOx-soot emissions trade-off for different payloads for the hybrid configurations as well as for the two baseline cases. All the cases studied with the hybrid configuration achieve EU VI NOx and soot conditions in the WHVC. In spite of the no-hybrid cases being out of the normative in some cases, the DMDF calibration allows to achieve the EU VI limits at engine-out levels in 0% and 50% of payload. This is not possible with the CDC calibration in any case. At full payload, the DMDF uses the top zone of the map (close to 350 hp), in which the soot emissions are large (see Figure 7b).

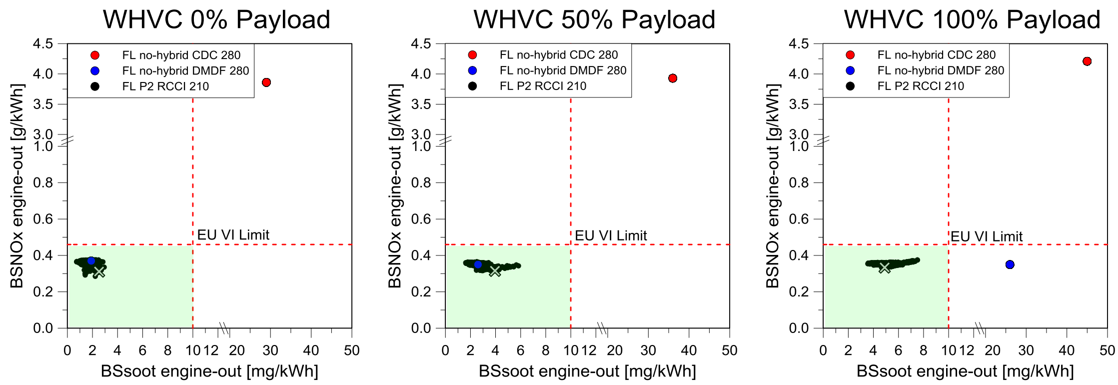

Figure 20 – Gear shift strategy for P2 FL 18-ton truck against the CO_2 reduction compared to CDC no-hybrid for 0% (a), 50% (b) and 100% (c) payload.

The FE platform corresponds to a medium-duty truck similar to the FL but with a maximum payload 7 ton higher than the aforementioned and additional axle and 12 transmission gear. Therefore, the maximum powertrain power increases up to 350 hp. Two versions were tested in this case, one with the RCCI 210 hp ICE map and other with the DMDF 280 hp ICE map. The objective to test both versions is to study the effect of increasing the maximum ICE power while decreasing the EM power output. The relation between both power sources is known as hybridization ratio (HR), calculated as the EM power divided by the total power. In the first case, the HR is 40% while in the second case the HR is 20%. In the FL truck, a unique value of 25% was used due to the no extra advantage of reducing the ICE power (see Figure 8).

Different to the small truck (FL-18 ton), the FE 25-ton truck shows limitations in terms of minimum gear strategy (Figure 21). For 100% payload, the minimum allowed value is 1400 rpm for the P2 DMDF 280 hp and 1820 rpm for the P2 RCCI 210 hp. This is mainly due to a lack of power from the ICE due to the mentioned rotational speed range (see Figure 8), which is not fully compensated by the electric machine. For these cases, it is possible to program a switchable control strategy dependent on the payload. However, a simple strategy is considered for this analysis, and the points that do not allowed the operation at 100% payload are discarded also as potential optimum values in the two other payloads. As seen in the previous truck analysis, the gear shift strategy has a strong impact on the fuel economy and CO_2 emissions.

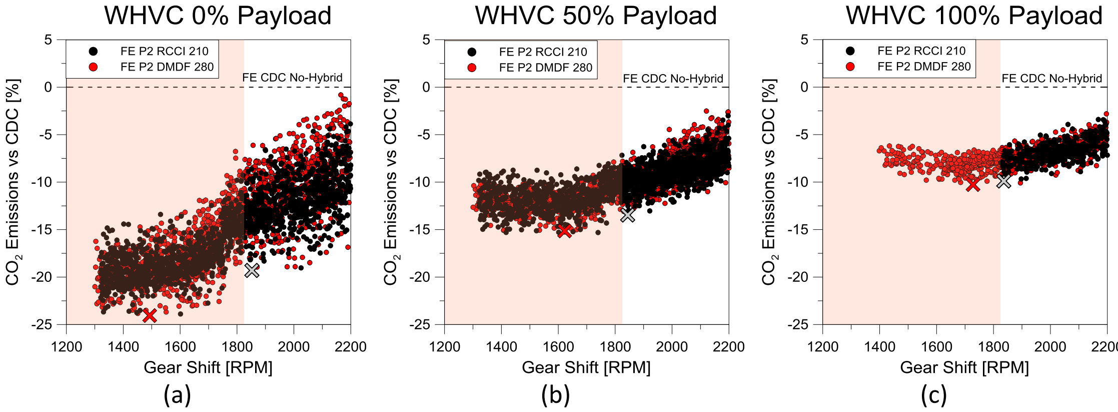

Figure 21 – Gear shift strategy for P2 FE 25-ton truck in versions RCCI 210 and DMDF 280 against the CO_2 reduction compared to CDC no-hybrid for 0% (a), 50% (b) and 100% (c) payload.

Figure 22 shows the battery effect on the CO_2 emissions reduction for the P2 FE 25-ton truck. The decrease of the electrification ratio from 40% to 20% allows to reduce the minimum allowed battery size from 16 kWh to 7 kWh (see Figure A2). For all the payloads, the increase of the battery size improves the powertrain efficiency due to lower thermal losses. This allows to improve the fuel economy/CO_2 emissions against the no-hybrid powertrain (dashed line). The dispersion of the points is similar between the two versions. It is important to note that, as in the previous truck, the payload has a direct effect on the CO_2 benefits. It is possible to achieve a reduction up to 25% with the empty truck, meanwhile with half and full payload this benefit is reduced to 15% and 10%, respectively. The other parameters included in the optimization are not showed for the brevity of the manuscript. The dependency of the CO_2 emissions against these parameters is soft as compared to the battery capacity and gear strategy.

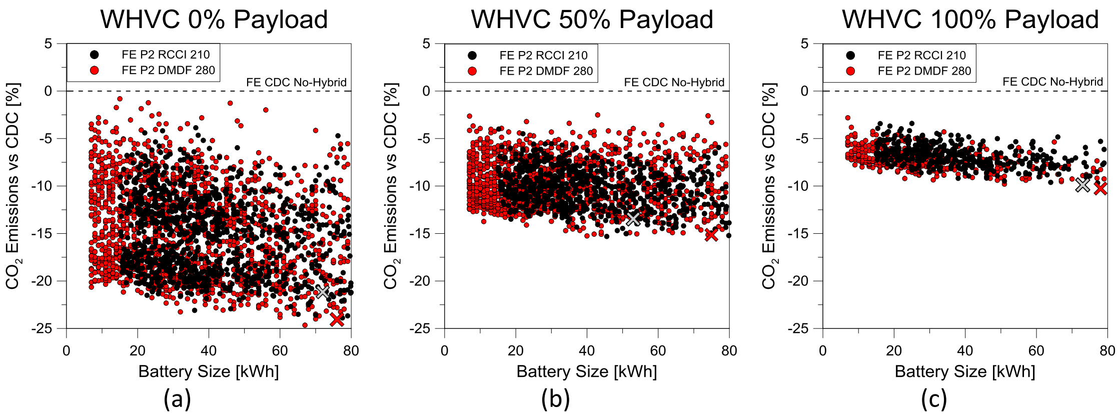

Figure 22 – Battery energy for P2 FE 25-ton truck in versions RCCI 210 and DMDF 280 against the CO_2 reduction compared to CDC no-hybrid for 0% (a), 50% (b) and 100% (c) payload.

One of the major problems of the DMDF 280 hp concept is the upper zone of the map, which is out of the EU VI normative in terms of soot emissions. In this zone, the values achieve a maximum of 300 mg/kWh, which is one order of magnitude higher than the normative. For this reason, the hybrid control needs to be tuned to allow a fuel consumption reduction with respect to the RCCI 210 hp, but without producing excessive particles matter. Figure 23a shows the NOx-soot trade-off at 50% payload and the baseline cases for the WHVC. The figures show that only a few cases can achieve the soot legislation levels for the DMDF 280 hp. In the case of RCCI 210 hp, all the cases show

EU VI legislation levels. Figure 23b shows a more detailed analysis with the trend between soot and CO_2 emissions for the FE MDF 280 hp at all conditions. There is a trade-off between CO_2 and soot that is more prominent at 50% payload. For the case of 0% payload, almost all the values are inside the normative while at 100% all the values are far from achieving this target. In the case of 50% payload, the configurations that enter inside the 10 mg/kWh soot target show an increase of CO_2 emissions of 7.5% as compared to the maximum possible gain. Therefore, it will be more beneficial to use a particle filter instead of trying to achieve the normative values at engine-out levels. For the FE DMDF case, the minimum CO_2 condition was selected. A cross mark is added in the graphs to identify the selection.

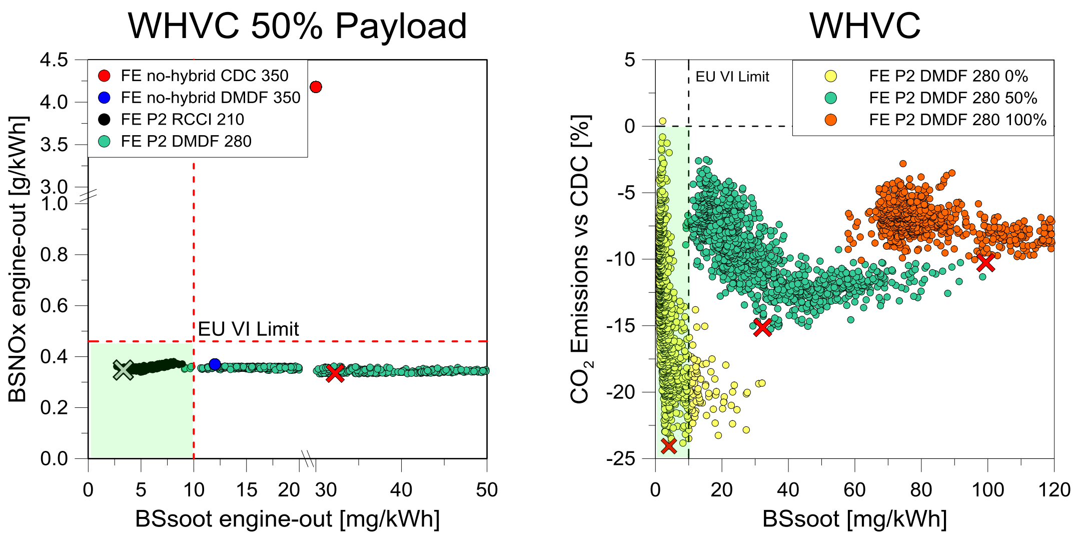

(a) (b)

Figure 23 – Nox-soot trade-off for different engine versions at 50% payload (a) and soot emissions aginst CO_2 emissions reduction for the DMDF 280 hp engine at different payloads (b).

4.2. Optimum selection by cost at 50% payload

After the analysis of the CO_2 emissions reduction potential of each hybrid truck platform and the discussion about the effect of using a RCCI or DMDF low temperature combustion on NOx and soot emissions, this section analyzes the effect of the battery cost to accomplish the right selection of the optimum case. Equation 1a is used to evaluate the CO_2 penalties and the battery cost. Figure 24 shows the penalties suffered by each truck platform for not achieving the 2025 CO_2 target (Equation 1b). The two FE P2 versions achieve the target with all the battery capacities studied in this work. On the other hand, as it is compared with the average fleet CO_2 emissions due to the new reference line, the FL P2 truck cannot achieve the CO_2 targets. As it is seen also for the no-hybrid case, the efficiency for the FL is lower than the FE due to the lower payload. The legislation considers the CO_2 emissions in ton per kilometer. In spite of this, the FL truck achieves important CO_2 reductions and the penalties decrease from 37.7 k€ to 2.4 k€ with medium size battery packages (30 kWh). The meaning of been below the zero penalties can be understand as a plus for the truck manufacturer in order to sell other vehicle with higher CO_2 emissions as the current no-hybrid platforms.

Figure 25 shows the penalties with the addition of the battery cost in the two scenarios. From the figure, it is possible to see the change in the trend observed in Figure

24, with more favorable results for low battery capacities. The reduction in the battery price from 2020 to 2025 leads to a decrease of the slope of the points. This graph shows the importance for the hybrid vehicles the reduction of the battery cost and weight with respect to the proposed EU penalties. The cross marks show the minimum cost function for each hybrid concept. From 2020 to 2025 the selection of the optimum in terms of cost does not vary for the FL RCCI 210. Low battery size (8 kWh) is preferred due to the low change in terms of CO_2 emissions with respect to the cost penalty. The FE RCCI 210 hp has a similar behavior without changes due to the battery cost. However, as the FE RCCI 210 equips a higher EM than the FL P2 RCCI, the optimum selection is in the mid-size range (50 kWh). Moreover, it is the FE DMDF 280 hp that achieves the best cost function in both battery cost scenarios. From 2020 to 2025, the battery selection changes from 11 kWh to 40 kWh. In the next section, these optimum cost cases are analyzed with other payloads (not only at 50% payload) and real driving cycles. For brevity of the manuscript, the 2020 battery cost scenario is analyzed. Lastly, Figure 25 shows that in both scenarios the use of hybrid technology covers the battery cost for the FE truck platform. This negative penalty can be seen as subside or plus for the company in order to meet the total fleet CO_2 targets.

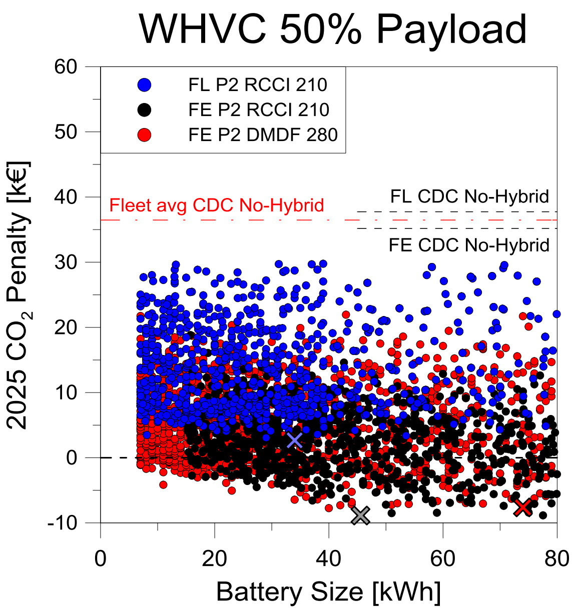

Figure 24 – CO_2 penalties for 2025 for the hybrid and no-hybrid platforms. The reference is the current fleet average from the study.

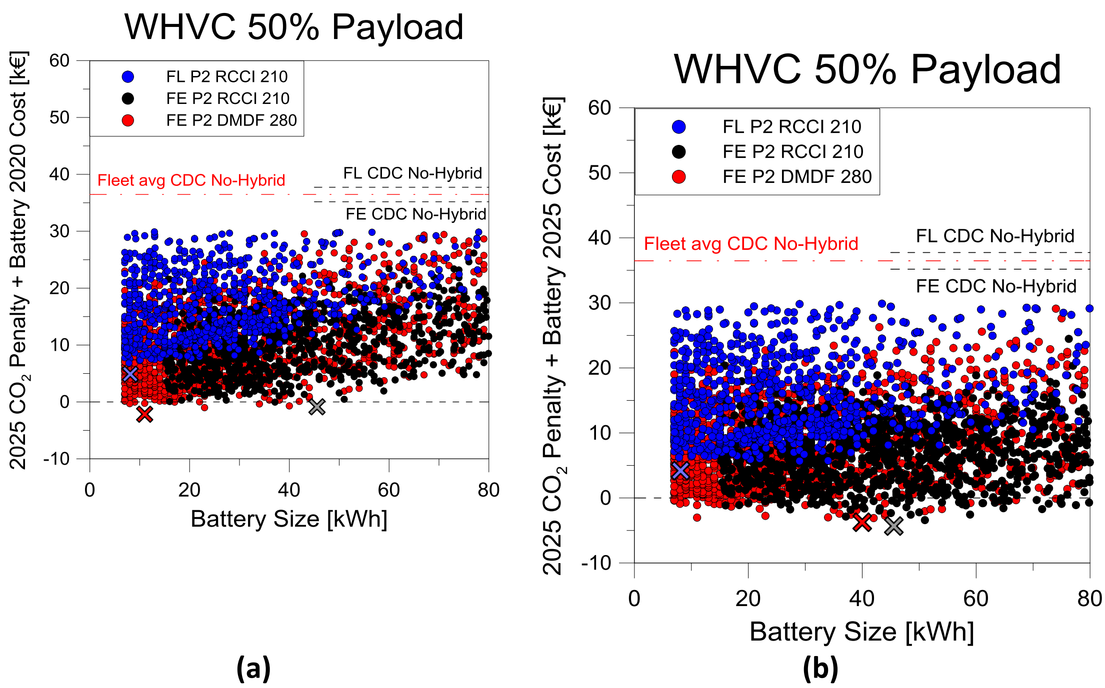

Figure 25 – CO_2 penalties and battery cost with two scenarios: Current battery cost (a) and 2025 battery cost (b).

4.3. Homologation and real driving cycles

The previously selected optimum CO_2 emissions and cost function are analyzed in all thre payload conditions and real driving cycles. All the results are compared to the CDC no-hybrid version in terms of percentage of reduction.

Figure 26 shows the CO_2 reduction of both optimum for the FL P2 RCCI 210 hp 18-ton truck with respect to the CDC 280 hp no-hybrid. The DMDF 280 hp no-hybrid baseline is also included in the graph for comparison. Figure 26 shows the results for the optimum selected in terms of CO_2 reduction, which includes a 34 kWh battery, and the optimum case selected considering the cost balance, which is equipped with a 8 kWh battery. For both cases, it is possible to observe that the urban case allows the highest CO_2 reduction (fuel economy) by far. The main reasons for this result are the high brake energy recovery potential and the improvement in terms of ICE operational points avoiding the idle operation by using the start-stop mode. On the contrary, the Local and Flat driving cycles achieve CO_2 reductions below 15% (EU target) for all the conditions due to the highest highway phase. The differences between both scenarios (CO_2 and cost selection) are below 1% in the total average, with 14.3% for the optimum CO_2 and 13.9% for the optimum cost. It is important to note that the no-hybrid DMDF produces a 0.6% CO_2 increase with respect to the CDC due to the lower average brake thermal efficiency of the ICE. The black circles depict the cases that achieve the EU CO_2 target for

2025. For both scenarios, almost half of the conditions tested achieve this target (5 of the 12 conditions).

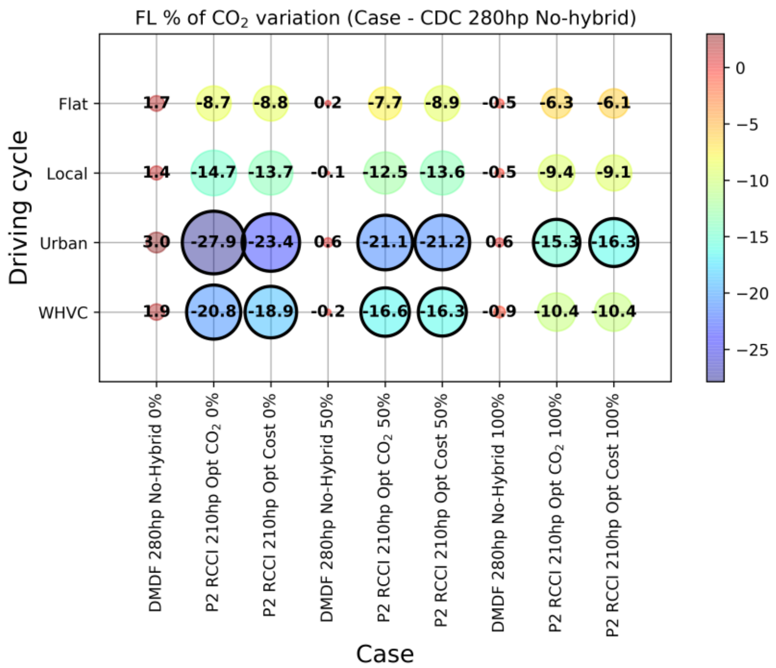

Figure 26 – CO_2 reduction for P2 RCCI 210 and DMDF no-hybrid with respect to CDC no-hybrid in different driving cycles and payload conditions with the best case for CO_2 reduction (AVG =-14.3%) and cost function (AVG = -13.9%) for FL 18-ton truck.

The engine-out NOx reduction obtained from the RCCI operation in the FL P2 truck allows that all the conditions achieve the EU VI levels. Figure 27a shows the percentage reduction with respect to the CDC case. For this truck platform, the DMDF 280 hp no-hybrid also achieves the EU VI level (0.46 g/kWh) with similar reduction than the hybrid case. Black circles highlight the cases that achieve the EU VI level. The situation for the soot emissions is different, in which the hybrid versions achieves the EU VI levels due to the full RCCI operation. On the other hand, the DMDF only to certain payload avoid the excessive soot particle emissions. At full load, the increase achieves up to 50% higher than the CDC. This is one of the main advantages of this de-rated RCCI version in the P2: it is possible to avoid the use of ATS for NOx and soot strongly decreasing the final price of the ICE platform. Due to the similarity of the results for the best CO_2 and cost reduction cases, only the first case was presented for the brevity of the manuscript.

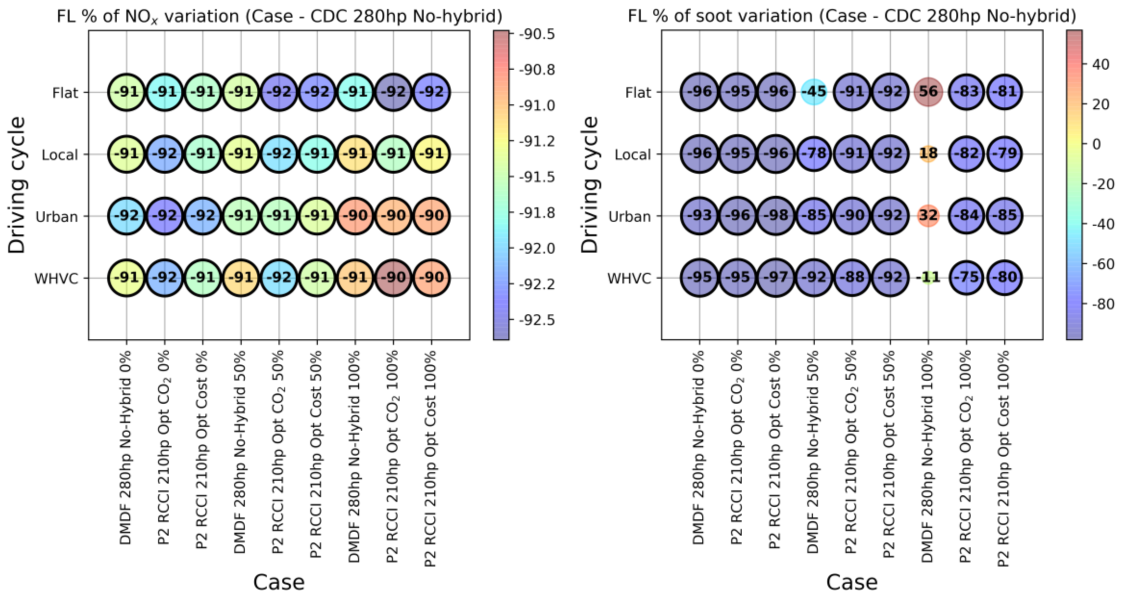

(a) (b)

Figure 27 - Emissions reduction for P2 RCCI 210 and DMDF 280 no-hybrid respect to CDC no-hybrid in different driving cycles and payload conditions with NOx (a) and soot (b) engine-out emissions for FL 18-ton truck.

The same analysis was done for the FE 25-ton truck. Figure 28 shows the optimum matrix for CO_2 reduction (Figure 28a) and cost balance (Figure 28b). The information is divided into two graphs because it is necessary to analyze the DMDF 280 hp and RCCI 210 hp hybrid versions. For the CO_2 optimum case and cost optimum case, the DMDF 280 hp shows a great advantage to reduce the greenhouse gases due to the large ICE operative range. This allows to reduce the gear strategy (Figure 21). The Urban continues being the most beneficial driving cycle for hybrid operation and the Flat is the worst. In average terms, the P2 RCCI 210 hp shows a 11.2% of reduction in the CO2 optimum case and 9.5% in the cost optimum case. On the other hand, the P2 DMDF 280 hp shows a reduction of 13.7% in the CO_2 optimum and 12% in the cost optimum case. Therefore, from these results it can be affirmed that the extended map range with the lowest hybridization ratio allows better CO_2 benefits.

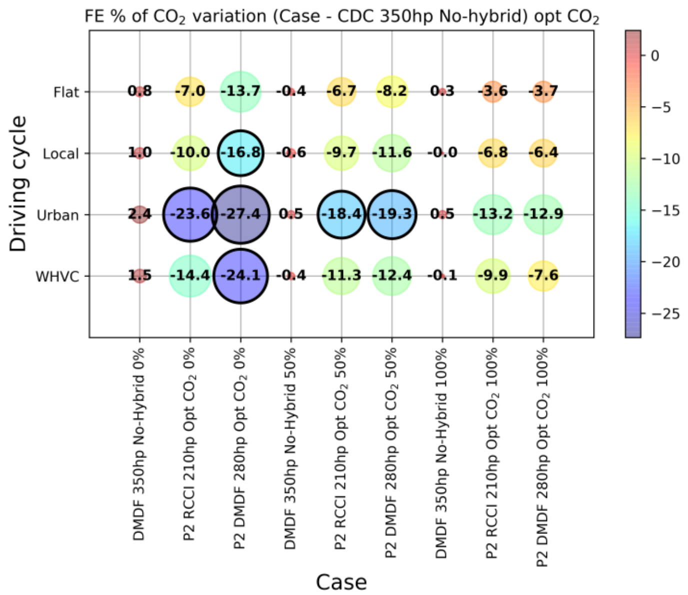

(a)

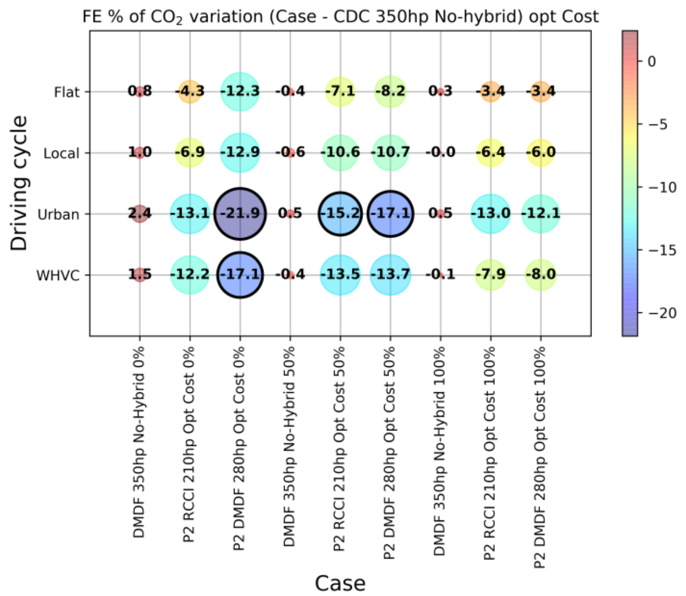

(b)

Figure 28 - CO_2 reduction for FE 25-ton truck in different driving cycles and payload conditions for: the optimum CO_2 reduction with P2 RCCI 210hp (AVG=-11.2%) and P2 DMDF 280hp (AVG=-13.7%) (a) and cost function P2 RCCI 210hp (AVG=-9.5%) and P2 DMDF 280hp (AVG=-12.0%) (b) with respect to CDC 350hp no-hybrid.

The NOx and soot emissions reduction against the CDC no-hybrid is depicted in Figure 29. The FE DMDF no-hybrid is included for reference. At engine-out levels, it is possible to observe that the LTC without hybridization does not achieve the EU VI NOx levels at 100% payload. This is because the use of the complete dual-fuel map. The P2 configuration achieves the EU VI NOx in all conditions for both combustion concepts (RCCI and DMDF). This demonstrates that, for advanced combustion modes, the hybridization is a possible way to achieve a full operation range avoiding the ICE operation at the highest loads. The soot emissions with the RCCI 210 hp are inside the EU VI as was the case of the FL platform. On the other hand, the DMDF 280 hp does not achieve the EU VI, with values at full payload that are 400% greater than the CDC and 300% greater than the DMDF no-hybrid. This is mainly due to the use of the most efficiency map zone (highest soot emissions) presented in the top of the DMDF 280hp map (Figure 7). A complete summary of the optimum selection is shown in Table 6.

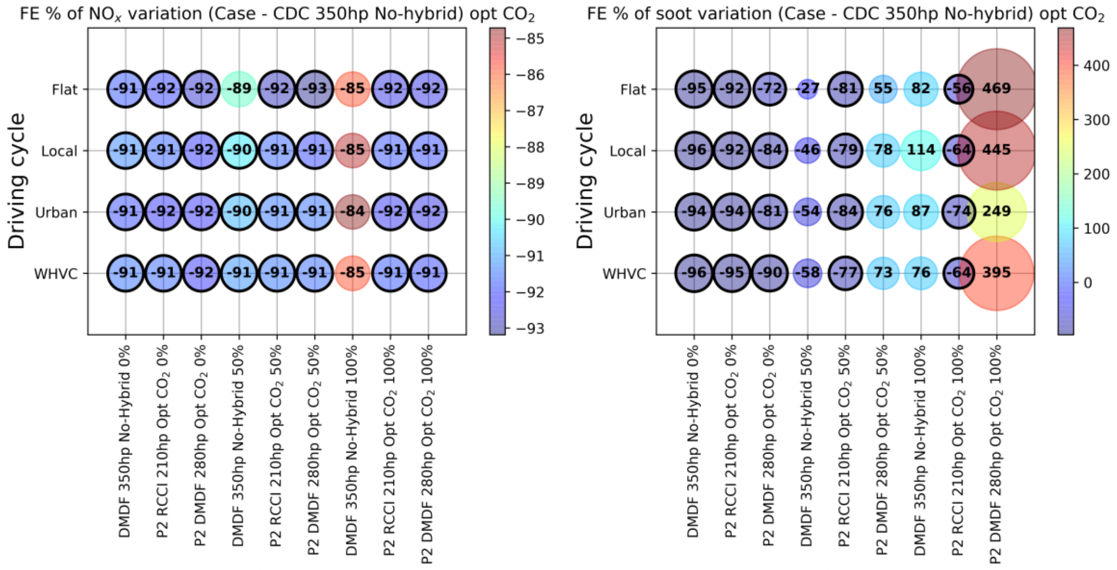

(a) (b)

Figure 29 - Emissions reduction for P2 RCCI 210, P2 DMDF 280 and DMDF 350 no hybrid with respect to CDC no-hybrid in different driving cycles and payload conditions with NOx (a) and soot (b) engine-out emissions for FE 25-ton truck.

Table 6 – Main hardware and control optimum parameters for the P2 RBC calibration.

Parameter	FL RCCI 210 CO_2	FL RCCI 210 Cost	FE RCCI 210 CO_2	FE RCCI 210 Cost	FE DMDF 280 CO_2	FE DMDF 280 Cost
Battery Energy [kWh]	34	8	73	45	74	11
Gear strategy [RPM]	1550	1330	1835	1845	1495	1695
Max. Speed EV mode [km/h]	64	7	29	17	85	40
Boost mode split [%]	86	1.5	90	1.5	36	3
SOC start charge [-]	0.50	0.56	0.56	0.52	0.56	0.56
SOC max charge [-]	0.52	0.48	0.55	0.51	0.49	0.52
Average CO_2 reduction vs CDC same truck [%]	-14.3	-13.9	-11.2	-9.5	-13.7	-12.0
$CO_{2@WHVC50\%}$ Reduction vs CDC same truck [%]	-16.6	-16.3	-11.3	-13.5	-12.4	-13.7
$CO_{2@WHVC50\%}$ Reduction vs OEM	-14.4	-14.1	-14.8	-17.0	-15.9	-17.2

average fleet [%]						
Cost Function 2020/2025 [k€]	8.6/5.6	4.7/4.1	4.5/-1.7	-0.9/-4.3	5.6/-0.4	-2.1/-3.0
$NOx_{@WHVC50\%}$ [g/kWh]	0.32	0.34	0.36	0.35	0.35	0.33
$soot_{@WHVC50\%}$ [mg/kWh]	4.0	2.7	6.8	3.3	51.8	31.1
$CO_{@WHVC50\%}$ [g/kWh]	5.0	6.3	6.1	6.3	5.9	6.2
$HC_{@WHVC50\%}$ [g/kWh]	2.4	3.2	2.6	2.9	2.7	2.7

5. Conclusions

Two medium-duty truck platforms with the ICE operating under low temperature dual-fuel combustion and with a hybrid electric powertrain were evaluated under homologation and real driving conditions. Three different payloads from empty to full payload were evaluated with a 0D vehicle model fed with experimental tests and validated against on-route measurements. Fuel consumption and emissions were estimated along the work with a map-based approach. The main findings were:

- Comparison with the commercial no-hybrid truck platform: The truck with the lowest payload (FL 18ton) achieves the highest CO_2 reduction in homologation conditions (WHVC and 50% payload). The FE 25 ton P2 was around 13% due to the better performance of the baseline compared with the FL 18 ton.
- Comparison with average OEM no-hybrid fleet: The truck with the highest payload (FE 25ton) achieves the highest CO_2 reduction due to the performance improvewhen the payload is increased. In the homologation case, the reduction achieved is 15.9% for the RCCI and 16.6% for the DMDF. The FE P2 hybrid achieves the European CO_2 target for 2025. The FL P2 was at 1% of CO2 reduction to achieve the desired target.
- The urban cycle was the most beneficial cycle with 30% and 15% CO_2 reduction for the empty truck and full payload conditions, respectively. On the other hand, driving conditions with large amount of highway decrease the benefits of the powertrain electrification with net gains below 10%.
- The NOx and soot emissions were other benefits of the proposed concept, with levels below the EU VI at engine-out for the FL-18 ton at all conditions using the RCCI 210 de-rated map and P2 70 hp EM. The FE-25 ton shows two alternatives: one with higher CO_2 benefits but soot above EU VI and the other with the RCCI 210 below the EU VI limits for both emissions.
- The cost function to evaluate the battery cost against the CO_2 penalties shows that with the current battery price, it is necessary to reduce the package to values below 10 kWh. On the other hand, the prices perspective and the continuous developing of the battery lithium-ion technology could

allow the selection of higher battery sizes to decrease the battery losses while not penalizing the cost.

Dual-fuel with hybrid electrified powertrain shows a large potential in order to meet the future emission legislations. It is important to note that CO and HC and cold start phases are one of the major disadvantages of LTC modes. It was not addressed in this article but it remains as future work with a complete analysis of the aftertreatment system performance.

Acknowledgments

The authors thanks ARAMCO Overseas Company and VOLVO Group Trucks Technology for supporting this research. The authors acknowledge FEDER and Spanish Ministerio de Economía y Competitividad for partially supporting this research through TRANCO project (TRA2017-87694-R). The authors also acknowledge the Universitat Politècnica de València for partially supporting this research through Convocatoria de ayudas a Primeros Proyectos de Investigación (SP20180148).

References

[1] Plötz P, Gnann T, Jochem P, Yilmaz HÜ, Kaschub T. Impact of electric trucks powered by overhead lines on the European electricity system and CO 2 emissions. Energy Policy 2019;130:32–40. doi:10.1016/j.enpol.2019.03.042.

[2] Smallbone A, Jia B, Atkins P, Roskilly AP. The impact of disruptive powertrain technologies on energy consumption and carbon dioxide emissions from heavy-duty vehicles. Energy Convers Manag 2020;6:100030. doi:10.1016/j.ecmx.2020.100030.

[3] Samsun RC, Krupp C, Baltzer S, Gnörich B, Peters R, Stolten D. A battery-fuel cell hybrid auxiliary power unit for trucks: Analysis of direct and indirect hybrid configurations. Energy Convers Manag 2016;127:312–23. doi:10.1016/j.enconman.2016.09.025.

[4] Wang E, Guo D, Yang F. System design and energetic characterization of a four-wheel-driven series-parallel hybrid electric powertrain for heavy-duty applications. Energy Convers Manag 2015;106:1264–75. doi:10.1016/j.enconman.2015.10.056.

[5] Sen B, Ercan T, Tatari O. Does a battery-electric truck make a difference? – Life cycle emissions, costs, and externality analysis of alternative fuel-powered Class 8 heavy-duty trucks in the United States. J Clean Prod 2017;141:110–21. doi:10.1016/j.jclepro.2016.09.046.

[6] García A, Monsalve-Serrano J, Martínez-Boggio S, Wittek K. Potential of hybrid powertrains in a variable compression ratio downsized turbocharged VVA Spark Ignition engine. Energy 2020;195:117039. doi:10.1016/j.energy.2020.117039.

[7] Liimatainen H, van Vliet O, Aplyn D. The potential of electric trucks – An international commodity-level analysis. Appl Energy 2019;236:804–14. doi:10.1016/j.apenergy.2018.12.017.

[8] Banjac T, Trenc F, Katrašnik T. Energy conversion efficiency of hybrid electric heavy-duty vehicles operating according to diverse drive cycles. Energy Convers Manag 2009;50:2865–78. doi:10.1016/j.enconman.2009.06.034.

[9] Mojtaba Lajevardi S, Axsen J, Crawford C. Comparing alternative heavy-duty drivetrains based on GHG emissions, ownership and abatement costs: Simulations of freight routes in British Columbia. Transp Res Part D Transp Environ 2019;76:19–55. doi:10.1016/j.trd.2019.08.031.

[10] Kim DM, Benoliel P, Kim DK, Lee TH, Park JW, Hong JP. Framework development of series hybrid powertrain design for heavy-duty vehicle considering driving conditions. IEEE Trans Veh Technol 2019;68:6468–80. doi:10.1109/TVT.2019.2914868.

[11] Mayet C, Welles J, Bouscayrol A, Hofman T, Lemaire-Semail B. Influence of a CVT on the fuel consumption of a parallel medium-duty electric hybrid truck. Math Comput Simul 2019;158:120–9. doi:10.1016/j.matcom.2018.07.002.

[12] Lajunen A. Fuel economy analysis of conventional and hybrid heavy vehicle combinations over real-world operating routes. Transp Res Part D Transp Environ 2014;31:70–84. doi:10.1016/j.trd.2014.05.023.

[13] Warey A, Bucknor N, Sutherland I, Potter M. An Exploratory Assessment of Electrified Propulsion Systems for Full-Size Heavy-Duty Truck Applications. SAE Tech Pap Ser 2019;1:1–7. doi:10.4271/2019-01-5002.

[14] Xu G, Jia M, Li Y, Chang Y, Liu H, Wang T. Evaluation of variable compression ratio (VCR)and variable valve timing (VVT)strategies in a heavy-duty diesel engine with reactivity controlled compression ignition (RCCI)combustion under a wide load range. Fuel 2019;253:114–28. doi:10.1016/j.fuel.2019.05.020.

[15] Pedrozo VB, May I, Guan W, Zhao H. High efficiency ethanol-diesel dual-fuel combustion: A comparison against conventional diesel combustion from low to full engine load. Fuel 2018;230:440–51. doi:10.1016/j.fuel.2018.05.034.

[16] Reitz RD, Duraisamy G. Review of high efficiency and clean reactivity controlled compression ignition (RCCI) combustion in internal combustion engines. Prog Energy Combust Sci 2015;46:12–71. doi:10.1016/j.pecs.2014.05.003.

[17] Kokjohn SL, Hanson RM, Splitter DA, Reitz RD. Fuel reactivity controlled compression ignition (RCCI): a pathway to controlled high-efficiency clean combustion. Int J Engine Res 2011;12:209–26. doi:10.1177/1468087411401548.

[18] Pachiannan T, Zhong W, Rajkumar S, He Z, Leng X, Wang Q. A literature review of fuel effects on performance and emission characteristics of low-temperature combustion strategies. Appl Energy 2019;251:113380. doi:10.1016/j.apenergy.2019.113380.

[19] Abdul-Manan AFN, Won HW, Li Y, Sarathy SM, Xie X, Amer AA. Bridging the gap in a resource and climate-constrained world with advanced gasoline compression-ignition hybrids. Appl Energy 2020;267:114936. doi:10.1016/j.apenergy.2020.114936.

[20] Sun R, Thomas RP, Tang X. HCCI Engine Application on a Hydraulic Hybrid Bus. SAE Int J Engines 2012;5:1581–94. doi:10.4271/2012-01-1631.

[21] Solouk A, Shakiba-Herfeh M, Arora J, Shahbakhti M. Fuel consumption assessment of an electrified powertrain with a multi-mode high-efficiency engine in various levels of hybridization. Energy Convers Manag 2018;155:100–15. doi:10.1016/j.enconman.2017.10.073.

[22] Benajes J, García A, Monsalve-Serrano J, Boronat V. Achieving clean and efficient engine operation up to full load by combining optimized RCCI and dual-fuel diesel-gasoline combustion strategies. Energy Convers Manag 2017;136:142–51. doi:10.1016/j.enconman.2017.01.010.

[23] Volvo T. VOLVO TRUCK SPECIFICATIONS n.d. https://www.volvotrucks.com/en-me/trucks/volvo-fl/specifications.html (accessed July 26, 2020).

[24] Benajes J, García A, Monsalve-Serrano J, Martínez-Boggio S. Optimization of the parallel and mild hybrid vehicle platforms operating under conventional and advanced combustion modes. Energy Convers Manag 2019;190:73–90. doi:10.1016/j.enconman.2019.04.010.

[25] Benajes J, García A, Monsalve-Serrano J, Martínez-Boggio S. Emissions reduction from passenger cars with RCCI plug-in hybrid electric vehicle technology. Appl Therm Eng 2020;164:114430. doi:10.1016/j.applthermaleng.2019.114430.

[26] García A, Carlucci P, Monsalve-Serrano J, Valletta A, Martínez-Boggio S. Energy management strategies comparison for a parallel full hybrid electric vehicle using Reactivity Controlled Compression Ignition combustion. Appl Energy 2020;272:115191. doi:10.1016/j.apenergy.2020.115191.

[27] Forgez C, Vinh Do D, Friedrich G, Morcrette M, Delacourt C. Thermal modeling of a cylindrical LiFePO4/graphite lithium-ion battery. J Power Sources 2010;195:2961–8. doi:10.1016/j.jpowsour.2009.10.105.

[28] Perez HE, Siegel JB, Lin X, Stefanopoulou AG, Ding Y, Castanier MP. Parameterization and Validation of an Integrated Electro-Thermal Cylindrical LFP Battery Model. Vol. 3 Renew. Energy Syst. Robot. Robust Control. Single Track Veh. Dyn. Control. Stoch. Model. Control Algorithms Robot. Struct. Dyn. Smart Struct., vol. 3, ASME; 2012, p. 41–50. doi:10.1115/DSCC2012-MOVIC2012-8782.

[29] Fischer H-M, Dorn L. Voltage Classes for Electric Mobility. Ger Electr Electron Manuf Assoc 2013:44.

[30] JSOL-Corporation. Motor design tool Jmag international 2020. https://www.jmag-international.com/express/ (accessed May 26, 2020).

[31] Eshani M, Gao Y, Gay S, Emadi A. Modern electric, hybrid electric and fuel cell vehicles 2nd. Edition. 2010. doi:10.1201/9781420037739.

[32] Luján JM, García A, Monsalve-Serrano J, Martínez-Boggio S. Effectiveness of hybrid powertrains to reduce the fuel consumption and NOx emissions of a Euro 6d-temp diesel engine under real-life driving conditions. Energy Convers Manag 2019;199:111987. doi:10.1016/j.enconman.2019.111987.

[33] Benajes J, García A, Monsalve-Serrano J, Martínez-Boggio S. Optimization of the parallel and mild hybrid vehicle platforms operating under conventional and advanced combustion modes. Energy Convers Manag 2019;190:73–90. doi:10.1016/j.enconman.2019.04.010.

[34] Benajes J, García A, Monsalve-Serrano J, Lago Sari R. Fuel consumption and engine-out emissions estimations of a light-duty engine running in dual-mode RCCI/CDC with different fuels and driving cycles. Energy 2018;157:19–30. doi:10.1016/j.energy.2018.05.144.

[35] Olmeda P, García A, Monsalve-Serrano J, Lago Sari R. Experimental investigation on RCCI heat transfer in a light-duty diesel engine with different fuels: Comparison versus conventional diesel combustion. Appl Therm Eng 2018;144:424–36. doi:10.1016/j.applthermaleng.2018.08.082.

[36] Benajes J, García A, Monsalve-Serrano J, Sari R. Clean and efficient dual-fuel combustion using OMEx as high reactivity fuel: Comparison to diesel-gasoline calibration. Energy Convers Manag 2020;216:112953. doi:10.1016/j.enconman.2020.112953.

[37] Xu G, Monsalve-Serrano J, Jia M, García A. Computational optimization of the dual-mode dual-fuel concept through genetic algorithm at different engine loads. Energy Convers Manag 2020;208:112577. doi:10.1016/j.enconman.2020.112577.

[38] Benajes J, Pastor J V., García A, Monsalve-Serrano J. An experimental investigation on the influence of piston bowl geometry on RCCI performance and emissions in a heavy-duty engine. Energy Convers Manag 2015;103:1019–30. doi:10.1016/j.enconman.2015.07.047.

[39] García A, Monsalve-Serrano J, Villalta D, Lago Sari R. Performance of a conventional diesel aftertreatment system used in a medium-duty multi-cylinder dual-mode dual-fuel engine. Energy Convers Manag 2019;184:327–37. doi:10.1016/j.enconman.2019.01.069.

[40] Bao R, Stobart R. Study on Optimization of Regenerative Braking Control Strategy in Heavy-Duty Diesel Engine City Bus using Pneumatic Hybrid Technology. SAE Tech. Pap., vol. 1, 2014. doi:10.4271/2014-01-1807.

[41] U.S. Department of Energy. Cost and Price Metrics for Automotive Lithium-Ion Batteries. Rep DOE/GO-102016-4908 2017:4.

[42] Benajes J, García A, Monsalve-Serrano J, Lago Sari R. Experimental investigation on the efficiency of a diesel oxidation catalyst in a medium-duty multi-cylinder RCCI engine. Energy Convers Manag 2018;176:1–10. doi:10.1016/j.enconman.2018.09.016.

Abbreviations

ATS	Aftertreatment sytems	hp	Horse Power
BEV	Battery electric vehicles	ICE	Internal combustion engine
BMEP	Brake mean effective pressure	LD	Light Duty
BSCO	Brake specific CO emissions	LI-Ion	Litium Ion batteries
$BSCO_2$	Brake specific CO_2 emissions	LTC	Low temperature combustion
BSFC	Brake specific fuel consumption	MD	Medium Duty
BSHC	Brake specific HC emissions	MHEV	Mild hybrid electric vehicle
BSNOx	Brake specific NOx emissions	NOx	Nitrogen Oxides
BSSoot	Brake specific soot emissions	OEM	Original equipment manufacturer
CDC	Conventional diesel combustion	P0	Belt alternator starter hybrid powertrain
CI	Compression Ignition	P1	Parallel hybrid electric vehicle without clutch
CO	Carbon Monoxide	P2	Parallel hybrid electric vehicle pre-transmission
CR	Compression ratio	P3	Parallel hybrid electric vehicle pos transmission
DI	Direct Injection	PHEV	Plug in electric vehicle
DMDF	Dual mode dual fuel	PM	particle matter
DOC	Diesel Oxidation Catalyst	PN	Particle number
DoE	Design of Experiments	RBC	Rule base control
DPF	Diesel particle filter	RCCI	Reactivity Controlled Compression Ignition
EM	Electric motor	rpm	Revolution per minute
EU	European Union	SCR	Selective Catalytic Reduction
FCEV	fuel cell vehicles	SI	Spark Ignition
FHEV	Full hybrid vehicle	SOC	State of the charge of the battery
GEN	Generator Motor	tkm	ton per kilometer
GHG	greenhouse gas emissions	TM	Traction Motor
HC	Unburned Hydrocarbons	TTW	Tank to wheel
HCCI	Homogeneous charge compression ignition	WHVC	World Harmonized Vehicle Cycle
HD	Heavy Duty	WTW	Well to wheel
HEV	Hybrid electric vehicle	ZEV	Zero Emission Vehicles

Appendix A

The cell uses to assembly the battery pack for the hybrid truck models is a cylindrical cell with 2.5 Ah each. The pack is selected to deliver 600v of nominal voltage by 181 series cells. The increase of parallel cells in the layout allows to increase the pack total capacity and energy. The battery size effect in power losses is presented in Figure A1. The calculation is performed for to EM size when discharge the maximum power. The curve behavior decreases exponentially with the increase of parallel cells. For the higher EM (140 hp) the power losses reduction in the battery change from 5% at 16 kWh to 0.9% at 80 kWh. This will improve the powertrain efficiency. Similar behavior is seen for EM of 70 hp.

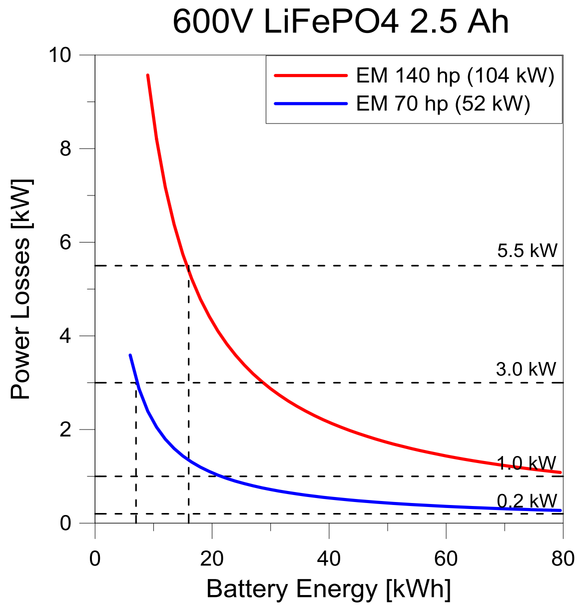

Figure A1- Battery losses for two electric machines (EM) size (140hp and 70hp) against different battery package size (battery energy/number of parallel cells).

For battery safety reasons, a control that limit the maximum voltage and current is added in the model. This limits the maximum power deliver to feed the EM and the maximum power absorbed to re-charge the batteries. Figure A2a show the voltage limit that is the most restrictive for charging. Figure A2b illustrates the current limit that is the most restrictive for discharge. Table 2 limits are used for the calculations. For battery sizing, the charging is used for limit the minimum energy allowed for the DoE optimization calculation. In case of using EM of 140 hp the minimum pack size is 16 kWh and for EM 70 hp is possible to use 7 kWh.

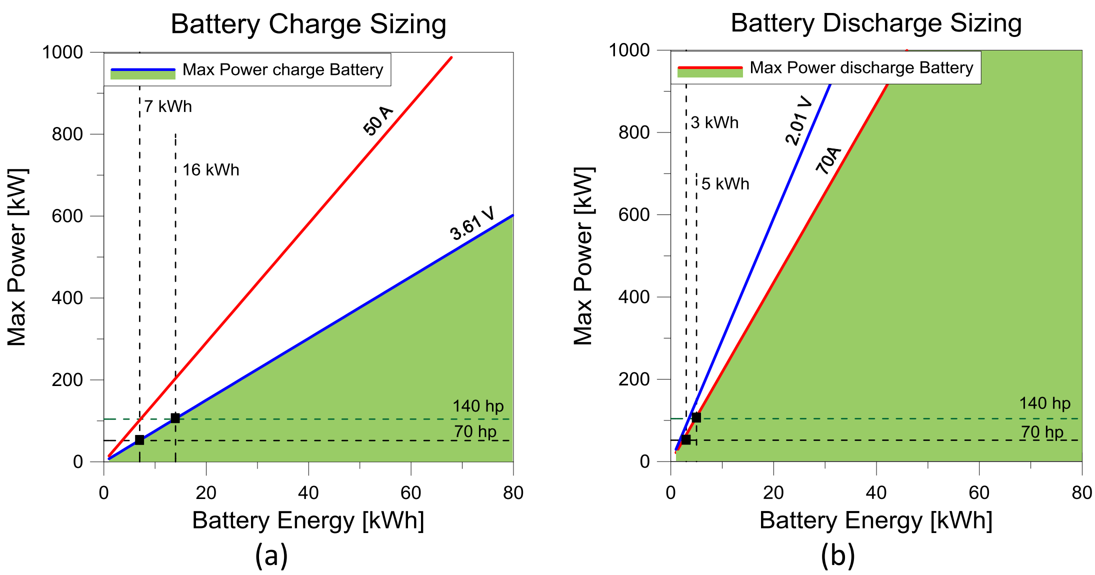

Figure A2 – Battery sizing with charge and discharge voltage and current limits for two electric machines (EM) size (140hp and 70hp).

Appendix B

Gasoline fraction (GF) and exhaust gas recirculation rate (EGR) are the key parameters to achieve an LTC. For the 6-cylinder engine calibration up to 93% of GF is used (mainly gasoline injection) and 55% of EGR rate as shows Figure B1. Figure B2 show the brake specific HC and CO emissions in the all engine map. This are important emissions that need to be estimated in order to size the DOC [42].

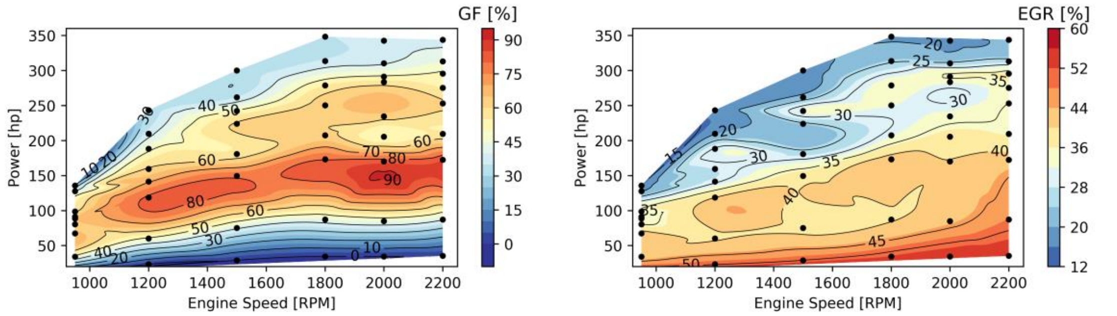

(a) (b)

Figure B1 – Gasoline fraction (GF) (a) and Exhaust gas recirculation rate (EGR) (b) calibration maps.

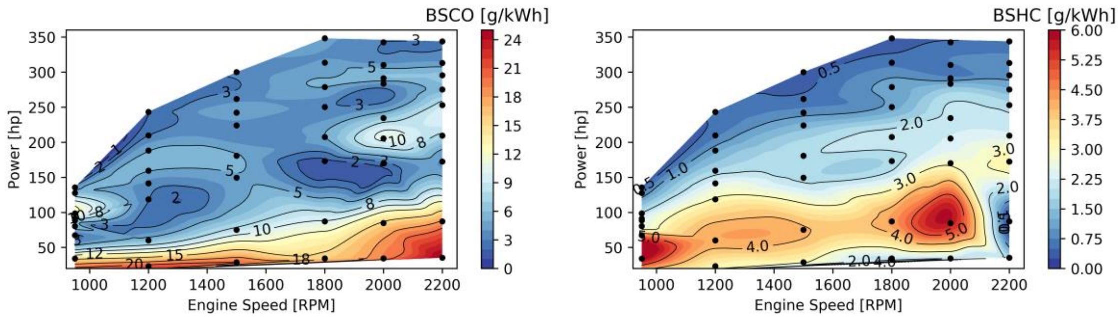

(a) (b)

Figure B2 - Brake specific CO emissions (a) and brake specific HC emissions (b) calibration maps.

Appendix C

The three-matrix explained in Figure 15 for the FL 18-ton hybrid truck is shown in Figure C1. The optimum of 0% (Figure C1a), 50% (Figure C1b), and 100% Figure C1c) payload is evaluated under 11 additional conditions. For this truck platform the optimization with 50% payload shows the best average results.

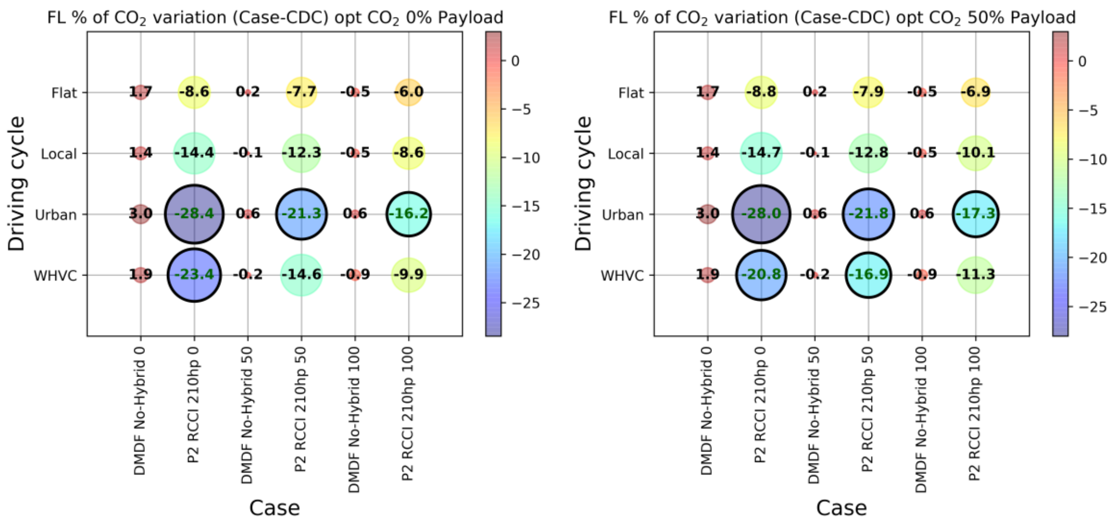

AVG Opt CO_2 0% = -14.2% AVG Opt CO_2 50% = -14.3%

(a) (b)

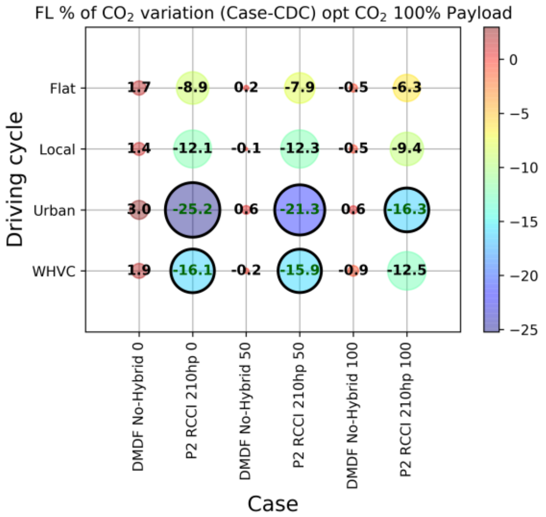

AVG Opt CO_2 100% = -13.7%

(c)

Figure C1 – FL 18-ton Truck optimization matrix for 0% payload CO_2 optimum (a), 50% payload CO_2 optimum (b) and 100% payload CO_2 optimum (c) in the 12 operative conditions.

Similar to the previous case, Figure C2 show the three-matrix for the FE 25-ton truck under the three optimums. In this case, two map concepts are presented. For the DMDF 280 the best case was seen by using the parameters of 0% payload. The main reason is the possibility to use low gear shift RPM change; therefore, benefits the empty truck operation with maximum of 27% of CO_2 reduction in urban and 24% in the WHVC. The RCCI 210 is more benefit with the calibration at 100% payload due to the restrictions in terms of gear shift.)

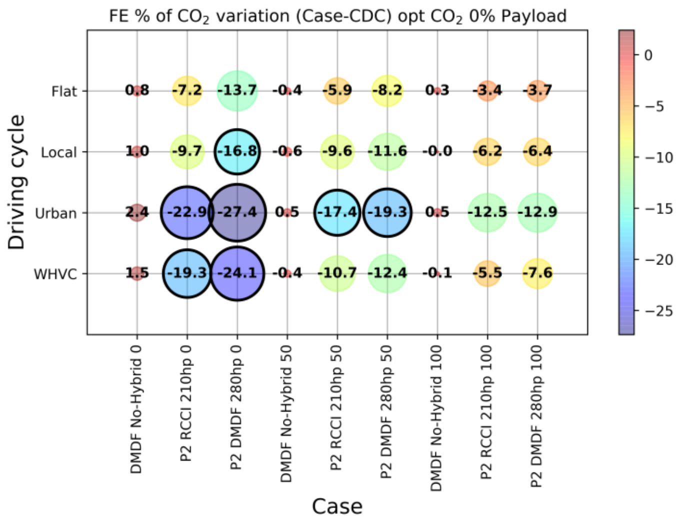

AVG RCCI Opt CO_2 0% = -10.8%; AVG DMDF Opt CO_2 0% = -13.7%

(a)

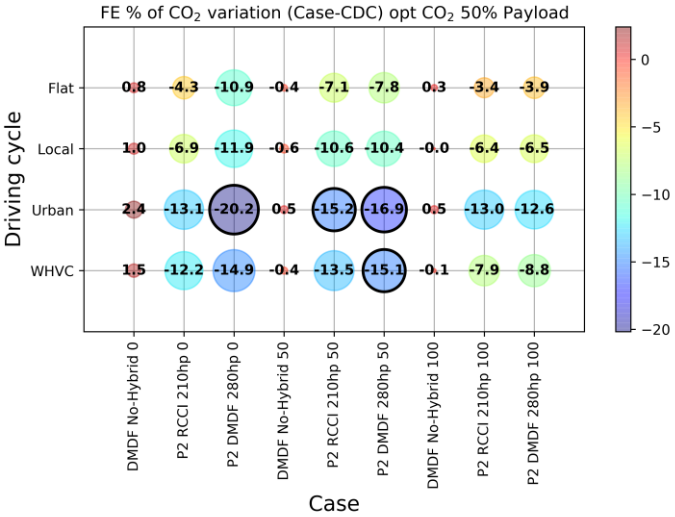

AVG RCCI Opt CO_2 50% = -9.5%; AVG DMDF Opt CO_2 50% = -11.7%

(b)

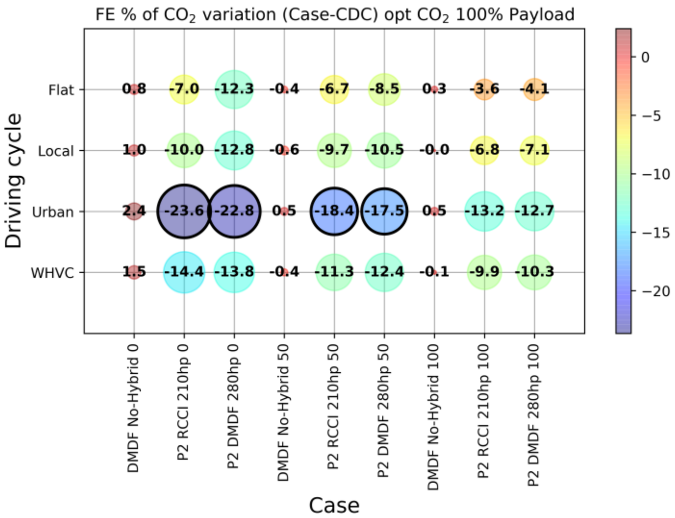

AVG RCCI Opt CO_2 100% = -11.2%; AVG DMDF Opt CO_2 100% = -12.1%

(c)

Figure C2 - FE 25-ton Truck optimization matrix for 0% payload CO_2 optimum (a), 50% payload CO_2 optimum (b) and 100% payload CO_2 optimum (c) in the 12 operative conditions.